Breast Cancer: Targets and Therapy

Dovepress
Taylor & Francis Group

Open Access Full Text Article

ORIGINAL RESEARCH

Dual Receptor Targeting Ensures Uptake and Anticancer Efficacy of Low-Density Lipoprotein-Docosahexaenoic Acid Nanoparticles Across Breast Cancer Cell Subtypes

Joseph Bower[1,2], Arnida Anwar[1], Jaideep Chaudhary[1,2], Zhe Chen[3], Marc Schumacher[4], Russell Debose-Boyd[4], Ian R Corbin[1,5,6]

[1]Advanced Imaging Research Center, University of Texas Southwestern Medical Center at Dallas, Dallas, TX, 75390, USA; [2]Simmons Comprehensive Cancer Center, University of Texas Southwestern Medical Center, Dallas, TX, USA; [3]Department of Biophysics, UT Southwestern Medical Center, Dallas, TX, 75390, USA; [4]Department of Molecular Genetics, University of Texas Southwestern Medical Center at Dallas, Dallas, TX, 75390, USA; [5]Department of Radiology, University of Texas Southwestern Medical Center at Dallas, Dallas, TX, 75390, USA; [6]Internal Medicine Division of Liver and Digestive Diseases, University of Texas Southwestern Medical Center at Dallas, Dallas, TX, 75390, USA

Correspondence: Ian R Corbin, Advanced Imaging Research Center, 5323 Harry Hines Blvd, Dallas, TX, 75390, USA, Tel +1 214-645-7044, Fax +1 214-645-2744, Email ian.corbin@utsouthwestern.edu

Introduction: Aberrant acquisition of lipoprotein cholesterol remains a hallmark feature of breast cancer biology. Low- and high-density lipoprotein receptors (LDLR and scavenger receptor class B type 1 (SR-B1)) are often upregulated to facilitate the tumor cells' high demand for cholesterol. To date, few attempts have been made to therapeutically exploit the high activity of lipoprotein receptors in breast cancer cells.

Methods: In the present study, we examined the utility of engineered low-density lipoprotein nanoparticles to deliver the natural anticancer omega-3 fatty acid docosahexaenoic acid (LDL-DHA) across a panel of breast cancer cells.

Results: Our data showed that LDL-DHA nanoparticles were avidly taken up (K_D 28 μg/mL to 1.9 μg/mL) and cytotoxic to all breast cancer subtypes (LD_{50} 52.2 μM to 4.7μM), with triple negative breast cancer cells showing some of the highest uptake and sensitivity to LDL-DHA. Follow-up receptor knockout studies in MDA-MB-231 cells revealed that LDL nanoparticle uptake is mediated by both LDLR and SR-B1. These receptors were shown to operate concurrently as well as in a compensatory manner to ensure ample uptake of LDL is maintained. Double knockout of LDLR and SR-B1 significantly impeded LDL nanoparticle uptake (<50%) and protected against LDL-DHA cytotoxicity (viability >70%).

Conclusion: In summary, our studies have shown that malignant cell dependence upon cholesterol acquisition can be exploited for lipoprotein–based drug delivery to breast cancer cells. Furthermore, the capacity of LDL nanoparticles to target both LDLR and SR-B1 ensures this as an efficient drug delivery platform against breast cancer cells.

Keywords: breast cancer, low density lipoprotein, docosahexaenoic acid, nanoparticle, multi-receptor

Introduction

Aberrant lipid metabolism is widely recognized as a critical process in breast cancer development and progression.[1–3] Dysregulated cholesterol homeostasis is one of the most widely documented perturbations of lipid metabolism in oncology, encompassing reports from both basic and clinical findings.[4,5] The dual nature of cholesterol to serve as both a driver[6] and nutrient[7] in cancer complicates the interpretation of epidemiological findings, such that a consistent association between serum cholesterol and breast cancer risk is difficult to conclude. The potential role of cholesterol as a driver of breast malignancy arises from its capacity to crosstalk with estrogen signaling pathways.[6] Cholesterol and its derivatives also play a role in breast cancer cell signaling by activating the estrogen receptor, estrogen-related receptors, hedgehog signaling, and G-protein-coupled receptors.[8–11] It would follow that having an abundance of cholesterol or its derivatives would be

Received: 17 July 2025
Accepted: 17 October 2025
Published: 6 December 2025

particularly beneficial for ER+ breast cancer, as the estrogen receptor is the main oncogenic driver in these tumors.[12] HER2+ and TNBC also benefit from the presence of cholesterol as many oncogenic drivers localize to lipid rafts, which are membrane domains composed of high concentrations of cholesterol and sphingolipids.[13–16] Induction of HER2 signaling is greatly enhanced when localized in these cholesterol-enriched rafts.[17] In the case of triple negative breast cancer, drivers such as EGFR, Pi3k, and AKT associate with lipid rafts to facilitate their oncogenic signaling.[14,18–21] While not innately oncogenic, lipid rafts do seem to play an essential role in oncogenic transformation, facilitating the clustering of various oncogenic proteins and drivers, thereby enabling coordinated oncogenic signaling.[22,23]

Cholesterol also serves as a principal nutrient in cancer, enabling a host of biological functions.[17,19,24] Cancer cells can acquire cholesterol through two pathways: sequestering exogenous cholesterol and de novo biosynthesis. In breast cancer, tumors that have higher expression of HMG-CoA reductase tend to be less aggressive.[25,26] Conversely, tumors that rely on acquiring cholesterol from their environment often disrupt circulating serum cholesterol homeostasis.[27–29] So much so that reports of hypocholesterolemia have been reported among patients with advanced malignancies.[30,31] These findings infer that as tumors grow, their need for cholesterol increases exponentially to sustain their growth.[31,32] It follows that low levels of serum cholesterol can be normalized with effective anti-tumor therapy, as demonstrated in breast cancer and other tumor types.[33]

Low-density and high-density lipoproteins (LDL and HDL) are primary transporters of cholesterol in mammalian systems.[34] As such, they are actively sequestered by malignant cells through the overexpression of LDL and HDL receptors to acquire cholesterol.[35,36] In fact, breast tumors that express higher levels of LDLR are more aggressive, and these patients experience shorter recurrence-free survival.[4,37] Similar relationships have been seen with the HDL receptor, as in vitro treatment of breast cancer cells with HDL has been shown to induce tumor cell proliferation.[38] In patients, tumors that express high levels of the HDL receptor, the Scavenger receptor class B type 1 (SR-B1), have more aggressive tumors and poorer prognosis.[39,40] Thus, tumors that rely on exogenous cholesterol demonstrate more aggressive biology, while those that rely solely on internal cholesterol synthesis trend towards less aggression. The current investigation aims to leverage the aforementioned perturbations in tumor lipid metabolism in a novel therapeutic approach against breast cancer. Our laboratory has engineered a novel biologic platform consisting of serum low-density lipoprotein (LDL) and the natural omega-3 polyunsaturated (PUFA) docosahexaenoic acid (DHA). We have previously demonstrated that this particle is able to elicit selective anticancer effects in hepatocellular carcinoma cell lines and preclinical models.[41,42] Omega-3 PUFAs are known to have significant anti-proliferative and apoptotic effects on breast cancer cells.[43,44] These natural fatty acids are cited to exert these effects through activation of multiple pro-apoptotic pathways that include but are not limited to: the regulation of Bac and Bcl-2 proteins; mitochondrial release of cytochrome c and the activation of caspases; cleavage of PARP; and PPAR-γ mediated upregulation of syndecan-1.[45–47] By exploiting the intrinsic sensitivity of breast cancer cells to omega-3 PUFAs and their dependence on cholesterol uptake, the LDL-DHA-based nanoparticle should enable a highly effective anticancer strategy against breast cancer cells.

Materials and Methods

Cell Lines and Cell Culture

Ten breast cancer cell lines were used, representative of the various subtypes of breast cancer. This panel included: MCF7 and T47D (Luminal A); ZR-75-1 and BT-474 (Luminal B); SKBR3 (HER 2 Enriched); MDA-MB-468 and HCC1937 (Basal Like); MDA-MD-231 and Hs578T (Claudin-Low); and SUM-149PT (Inflammatory breast cancer). Cells were cultured as follows: MCF7 and Hs578T lines were cultured in Dulbecco's Modified Eagle Medium, DMEM (Sigma #D6429) supplemented with 10% fetal bovine serum and 1% penicillin/streptomycin. MDA-MB-231s, including knock-out derivatives, MDA-MB-468, ZR-75-1, T47D, and HCC1937 cell lines were cultured in RPMI 1640 (Sigma #R8758) supplemented with 10% fetal bovine serum and 1% penicillin/streptomycin. SKBR3 and BT474 cells were cultured in RPMI 1640 supplemented with 10% FBS, 15mM HEPES, and 1% Penicillin Streptomycin. SUM149PT cells were cultured in F12 Nutrient Mixture (Ham) (Gibco #11765-054) supplemented with 10% FBS and 1% penicillin and streptomycin. Chinese hamster ovary (CHO) cells: CHO-K1 (subclone derived from the parental line), LDLA7 (LDL receptor-negative) and LDLA mSR-B1 (murine SR-B1 transfected into ldlA cells) were cultured in DMEM-F12 media

(Hyclone #SH30023.02) supplemented with 5% FBS and 1% Penicillin/Streptomycin. Once at confluency, cells were subcultured by washing with PBS (Sigma #D8367) and treatment with Trypsin-EDTA 0.25% (Sigma #T4049) and inactivation of trypsin by overdose of complete media. Cell lines had institutional review board approval by the University of Texas Southwestern Institutional Animal Care and Use Committee (IACUC)).

Low-Density Lipoprotein (LDL), High-Density Lipoprotein (HDL) Isolation and Nanoparticle Formulation

Human LDL was isolated from apheresis plasma of patients with familial hypercholesterolemia using sequential density gradient ultracentrifugation as described previously by Lund-Katz et al.[48] HDL was isolated from normal human plasma also by sequential density gradient ultracentrifugation[49] and further purified by apoB depletion.[50] The collected HDL was then used for inhibition studies.

LDL-DHA and LDL-DiI-OA particles were created as previously described by Mulik et al.[51] Briefly, LDL freeze-dried in the presence of starch was subject to several rounds of organic extraction to remove nonpolar lipids from LDL. Thereafter, DHA or DiI and OA (dissolved in heptane) were added to the LDL residue and incubated at 4°C for 90 min. Heptane was then removed by nitrogen gas, and the sample was re-suspended in 10 mM tricine buffer. Finally, the sample was clarified by low-speed centrifugation and stored under N2 atmosphere at 4°C.

Fluorescent DiI labelled LDL and HDL were prepared by incubating the lipophilic carbocyanine dye with LDL or HDL at a molar ratio of 82:1. The reaction was carried out at 37°C for 18 h, followed by removal of excess label using ultracentrifugation (49,000 rpm for 20 h at 4°C).[52]

Characterization

Physicochemical characterization (structure and composition) of the LDL nanoparticles was performed as described previously[53] to assess particle size and polydispersity (dynamic light scattering), surface charge (zetapotential), and composition (protein assay and liquid chromatography mass spectrometry) to ensure consistency of batch to batch preparations.

CryoTEM Imaging

Three to four microliters of the LDL nanoparticle solution were added to Lacey carbon grids (300-mesh; Ted Pella, Inc.) that were negatively glow-discharged for 80 seconds at 30 mA. Excess sample was removed by blotting once for 3 seconds with Vitrobot filter paper (Ted Pella, Inc) and then the grid was plunge-frozen in liquid ethane cooled by liquid nitrogen using a Vitrobot plunge-freezer (ThermoFisher Scientific).

The vitrified LDL nanoparticle samples were imaged using a Talos Arctica 200 kV transmission electron microscope (ThermoFisher Scientific) equipped with a Gatan K3 camera (Gatan, Inc). The SerialEM software was used to collect images under low-dose conditions at 36,000x or 45,000x magnification corresponding to a pixel size of 1.14 Å/pixel or 0.88 Å/pixel, respectively. For each image, 50 frames were recorded over 2.5 second exposure time at a dose rate of 35 electrons/pixel/s. The movie frames were aligned using MotionCor2.[54] MotionCor2: anisotropic correction of beam-induced motion for improved cryo-electron microscopy.[55] After alignment, images were further processed for contrast using EMAN2 and scale bars were added using FIJI.[56]

Western Blotting

Cells were lysed using cell lysis buffer (Cell Signaling #9803) supplemented with cOmplete Mini, EDT-Free protease inhibitor cocktail (Roche #11836170001). Lysed cells were then centrifuged at 21000 RCF for 10 minutes. Protein concentration was measured by BCA Assay (Thermo Scientific #23227). Samples were prepared with even protein concentration and 6X Laemmli SDS sample buffer (Alfa Aesar #J61337-AC). Samples were resolved on 4–20% Gel (Biorad #4561096). Transfer was done using a preassembled kit with a PVDF membrane (Biorad #1704157). Portions of the membrane to be immunoblotted for LDLR were blocked with 5% nonfat skim milk. All other parts of the membrane were blocked using 1X Casein Blocking Buffer (Sigma #B6429) in TBS with 0.01% Tween 20. Primary Antibody

Incubations were done overnight at 4°C with gentle shaking. The LDLR antibody was a gift from Joachim Herz and was used at a 1:1000 dilution. Anti-SR-B1 antibody was from Novus (#NB400-104). Actin Antibody was from Santa Cruz (#sc-8432).

LDL-DHA Dose Response

All cell lines were plated in a 96 well plate at a density to reach 80–90% confluence after one day. The next day cells were serum-starved with RPMI 1640 and incubated overnight. The following day, cells were treated with a dose range of 5–100 uM LDL-DHA. Cell viability was determined 72 hours later by incubating cells for 1 hour with CCK8 reagent (Dojindo #CK04-20) diluted 10-fold in RPMI 1640. Absorbance was measured at 450 nm on a ThermoMax plate reader (Molecular Devices). Survival was calculated as total survival normalized to untreated control cells.

LDL-DiI and LDL-DiI-OA Uptake and Inhibition

All cell lines were treated as follows. First, cells were plated in a six-well plate at 5×10^5 cells per well and left to attach overnight. All cells were then starved of serum in RPMI 1640. Cells were then incubated with LDL-DiI or LDL-DiI-OA for 6 hours. After nanoparticle incubation, cells were washed with PBS, then harvested with trypsin-EDTA and inactivated with complete media. Cells were then pelleted by centrifugation at 200 RCF, and trypsin-media mixture was removed by careful aspiration. Cells were then resuspended in PBS and taken to the UTSW flow cytometry core, and fluorescence was measured on a FACSCalibur machine (BD Bioscience) with excitation 488nm and emission at 585 nm. Data analysis was performed with FlowJo 10 (BD Bioscience) and GraphPad Prizm 7 (GraphPad Software).

Uptake inhibition proceeded much the same, except that after serum starvation, cells were incubated for one hour with 20 ug of SR-B1 antibody (Novus #NB400-113) or 200 ug LDL, 200 ug HDL, and an excess of 200 ug LDL and 200 ug HDL. Cell harvesting and data collection proceeded in the same manner.

Knockouts of LDLR and SR-B1

MDA-MB-231 cells were transfected with jetPRIME (Polyplus Transfection #114-01) to insert either of the following plasmids (LDLR knockout #sc-400645-KO-2 or SR-B1 knockout #sc-400990). Twenty-four hours after transfection, cells were washed with PBS, treated with trypsin-EDTA and trypsin was inactivated with complete media. Cells were then centrifuged at 200 RCF, and the media was carefully aspirated. Cells were then resuspended in complete media and were taken to the UTSW flow core to be sorted under aseptic conditions based on GFP expression on a FACSAria III (BD Bioscience) into a 96 well plate with 1 cell per well. Cells were amplified and screened for LDLR or SR-B1 expression. For the shRNA Knockdown of SR-B1 LDLR CRISPR knockout MDA-MB-231 cells were infected with a virus obtained from Peter Michaely at UT Southwestern. Virus was co-infected with 5 ug/mL polybrene (Millipore #TR-1003-G). Virus infection was allowed to occur for 48 hours thereafter, cells were passaged and selected with 5ug/mL puromycin (Alfa Aesar #AAJ67236XF) for 1 week. After the selection, cells were expanded, and expression of LDLR and SR-B1 was measured by Western blot as described.

Confocal Fluorescent Microscopy

Cells were seeded on 35mM confocal dishes (MatTek Corporation #NC9268399) and allowed to recover overnight. The following day, cells were serum-starved using RPMI1640 with no supplements. On the third day, cells were treated with equal amounts (based on DiI content) of LDL-DiI, LDL-DiI-OA, or HDL-DiI for 3 hours. Two hours after lipoprotein-DiI treatment, cells were incubated with 1.33 μM LysoSensor green (ThermoFisher #L7535). Cells were then washed with PBS, and fresh starvation media were added. Cells were then imaged by Z-Stack using a Zeiss LSM 780 Inverted microscope. All images were taken using the 63X objective lens. Image processing was then done using FIJI.

qRT-PCR Expression of Cholesterol Pathway Genes

MDA-MB-231 wild-type and knockout cells were plated in a 10 cm dish and left in normal media, or serum starved as indicated. Cells were washed once with PBS, then harvested with 1 mL Trizol. RNA extraction was performed according to the manufacturer's instructions. Equal amounts of RNA from individual cells were treated with DNase I (DNA-free,

Ambion/Life Technologies, Grand Island, NY). First-strand cDNA was synthesized from 10 µg of DNase I-treated total RNA with random hexamer primers using TaqMan Reverse Transcription Reagents (Applied Biosystems/Roche, Branchburg, NJ). Specific primers for each gene were designed using Primer Express software (Life Technologies) or the Primer Bank of Harvard University. The real-time RT-PCR reaction was set up in a final volume of 20 µL containing 20 ng of reverse-transcribed total RNA, 167 nM of the forward and reverse primers, and 10 µL of 2X SYBR Green PCR Master Mix (Life Technologies). PCR reactions were done in triplicate using ViiA7 Applied Biosystems. The relative amount of all mRNAs was calculated using the comparative threshold cycle (CT) method. GAPDH mRNA was used as the invariant control. Sequences for primers used for qRT-PCR are listed in Supplementary Information.

Lipid Peroxidation and Annexin V/Propidium Iodide FACS

Cells were seeded to reach 80–90% confluence after 24 hours in a 6 well plate and allowed to attach. The following day, cells were serum-starved with RPMI 1640 and incubated overnight. At this point, cells were treated with various doses of DHA, and cells destined for lipid peroxidation assay were also treated with Bodipy-lipid. Cells treated for lipid peroxidation were harvested with trypsin and then taken to the UTSW flow cytometry core and fluorescence was measured on a FACSCalibur machine (BD Bioscience). Processing was then done with Flowjo, and the mean fluorescence intensity for FL1 and FL2 was calculated, then the ratio of FL1/FL2 was taken for each sample. The ratio for each sample was then divided by the ratio of a control sample that was untreated with LDL-DHA to obtain the increase or decrease in lipid peroxidation for each sample.

Cells destined for the apoptosis assay were harvested with trypsin, then spun at 300 RCF for 5 minutes and processed according to the manufacturer's instructions for the TACS Annexin V-FITC apoptosis detection kit (R&D Systems #4830-250-K). Cells were then measured on FACSCalibur, with processing then done in FlowJo to determine the apoptotic or necrotic state of the cell.

Caspase Activity Assay

Cells were seeded in 96 well plates and grown to 85% confluency, followed by serum starvation overnight. Cells were then treated with LDL-DHA or Ionosporine or Staurosporine for 8 hours at 37°C. Caspase activation and viability were determined using ApoLive-Glo™ Multiplex Assay (Promega Cat# G6410). The caspase activity signal was divided by the viability signal to normalize for caspase activity from live cells.

qRT-PCR Expression of Antioxidant Genes

Select BRCA cell lines (MDA-MB-231, HCC1937 and MCF7) were grown in 6-well plates up to 90% confluency, followed by overnight serum starvation. Collected cells were then processed as described for examination of the cholesterol pathway genes. Sequences for primers used for qRT-PCR are listed in Supplementary Information.

Statistical Evaluation

The results were expressed as mean ± standard error. Analysis of variance (ANOVA) with Tukey's multiple comparison post hoc testing was used for the evaluation of differences between groups. Differences with a P value less than 0.05 were deemed significant.

Results

Lipoprotein-Based Nanoparticles

The engineered LDL, nanoparticles loaded with unesterified DHA were produced by the reconstitution method. The nanoparticles' physicochemical characteristics (Table 1) were in keeping with previous preparations. Size measurements (via dynamic light scattering) showed that on average, the diameter of the LDL-DHA nanoparticles was 21.2 ± 4.2 nm, and an electronegative zeta potential reading (−24.5 ± 6.9 mV) was reported. Plasma LDL, which serves as a control nanoparticle, was similar in size to LDL-DHA (20.0 ± 1.1 nm), but displayed a more neutral zeta potential (~-9.0±1.8 mV). Flurophore-labelled LDL nanoparticles were also prepared by incubation (LDL-DiI) and reconstitution (LDL-DiI-

Table 1 Lipoprotein Nanoparticles. Characterization Table Containing Physicochemical Properties and Lipid or Dye Loading of Plasma LDL, LDL-DiI, LDL-DHA, LDL-DiI-OA and HDL-DiI Nanoparticles

Parameter	Plasma LDL	LDL-DiI	LDL-DHA	LDL-DiI-OA	HDL-DiI
Diameter (nm)	20.00 ± 1.08	20.32 ± 2.95	21.20 ± 4.22	20.2 ± 3.420	9.45 ± 0.41
Zeta Potential (mV)	−9.01 ± 1.82	−8.54 ± 1.08	−24.50 ± 6.99	−29.3 ± 1.08	−0.8 ± 5.21
DiI Dye (ng/mL)	ND	40682 ± 6316	ND	42496 ± 6946	1555 ± 241
DHA content (mM)	*	ND	7.01 ± 3.05	ND	*

Notes: * DHA typically makes up only 1% and 2% of the total fatty acid composition of LDL and HDL, respectively.
Abbreviation: ND, not determined.

OA) methods. Fluorescent LDL-DiI and LDL-DiI-OA, which served to track the activities of native LDL and LDL-DHA, contained 40682 ± 6316 and 42496 ± 6946 ng/mL of DiI, respectively. Physicochemical characteristics that include nanoparticle diameter (20.3 ± 2.9 and 20.2 ± 3.4 nm) and zeta potential (−8.5 ± 0.3 and −29.3 ±7.9 mV) were also, respectively, documented for the LDL-DiI and LDL-DiI-OA nanoparticles. Finally, fluorescent DiI labelled HDL was also prepared by the incubation method. These particles were 9.5 ± 0.4 nm in diameter and displayed a near-neutral zeta potential (−0.80 ± 5.2 mV). DiI loading on the HDL was on average 1555 ng/mL.

LDL-DHA Nanoparticles Kill All Subtypes of Breast Cancer

To evaluate the anticancer cytotoxicity of LDL-DHA nanoparticles, we performed an MTS cell viability assay across our panel of breast cancer cells. Figure 1 shows the dose response at 72 hours to LDL-DHA for MCF7 (1A), T47D (1B), ZR-75-1 (1C), BT-474 (1D), SKBR3 (1E), MDA-MB-468 (1F), HCC1937 (1G), MDA-MB-231 (1H), Hs578T (1I) and SUM-149PT (1J). The calculated median lethal dose (LD_{50}) of LDL-DHA was as follows: MCF7, 39.05 μM; T47D, 44.34 μM; ZR-75-1, 30.46 μM; BT-474, 52.23 μM; SKBR3, 29.78 μM; MDA-MB-468, 14.9 μM; HCC1937, 14.61 μM; MDA-MB-23, 14.9 μM; Hs578T, 6.05 μM; SUM-149PT, 4.70 μM) (see Supplementary Table 1). A marked difference in sensitivity between hormone responsive cell lines (Figure 1A–E) and triple negative (Figure 1F–J) was noted.

Lipoprotein Receptors Facilitate LDL-DHA Uptake

To examine the contributions of receptor-mediated uptake to the LDL-DHA cytotoxicity, we embarked on mechanistic uptake studies in MDA-MB-231 cells, one of the most commonly studied breast cancer cell lines. Anticipating that LDLR would be the predominant transporter of LDL nanoparticles into the cell, we generated LDLR CRISPR knockout MDA-MB-231 cell line (MDA-MB-231 LDLR-/-) (Figure 2A). Uptake studies with LDL-DiI particles in the MDA-MB-231 LDLR-/- cells followed, showing complete blockade of LDL-DiI (Figure 2B). Next, we moved to examine the LDL-DHA dose response of the MDA-MB-231 LDLR-/- cells and were surprised at the lack of rescue from LDL-DHA cytotoxicity (Figure 2C). The discordant finding between inhibited uptake of LDL-DiI and the persisting cytotoxicity of LDL-DHA in the MDA-MB-231 LDLR-/- cells led us to consider the differences between these nanoparticles. The electronegative surface charge and bilayered phospholipid organization of LDL-DHA are not reflected in the LDL-DiI particle which has a neutral surface charge and has a phospholipid monolayer/cholesterol core structure (Table 1) (Supplementary Figure 1).[51] As such, LDL-DiI-OA, which bears similar physicochemical properties and structural organization as LDL-DHA (Supplementary Figure 1) was employed for evaluation of uptake studies with MDA-MB-231 LDLR-/-.

Following incubation with the LDL-DiI-OA particle, the MDA-MB-231 LDLR-/- cells were able to readily take up this particle to a similar level as wild-type MDA-MB-231 cells (Figure 2D). This result suggested that the LDL-DiI-OA (and LDL-DHA) nanoparticles could be internalized into cells other than the LDLR pathway. An alternate lipoprotein-cholesterol sequestering receptor pathway is the high-density lipoprotein (HDL) receptor, scavenger receptor class B type 1 (SR-B1). Previous studies support this notion in suggesting that LDL and LDL-modified particles can bind/interact with the multi-ligand receptor SR-B1.[57,58] Interestingly, Western blot analysis of the MDA-MB-231 cells revealed an upregulation of SR-B1 expression in the MDA-MB-231 LDLR-/- cells relative to wild-type cells. To further investigate this interaction, we acquired the Chinese hamster ovarian cell lines, CHO-K1, ldlA7 and ldlA7[mSR-B1]. The CHO-K1

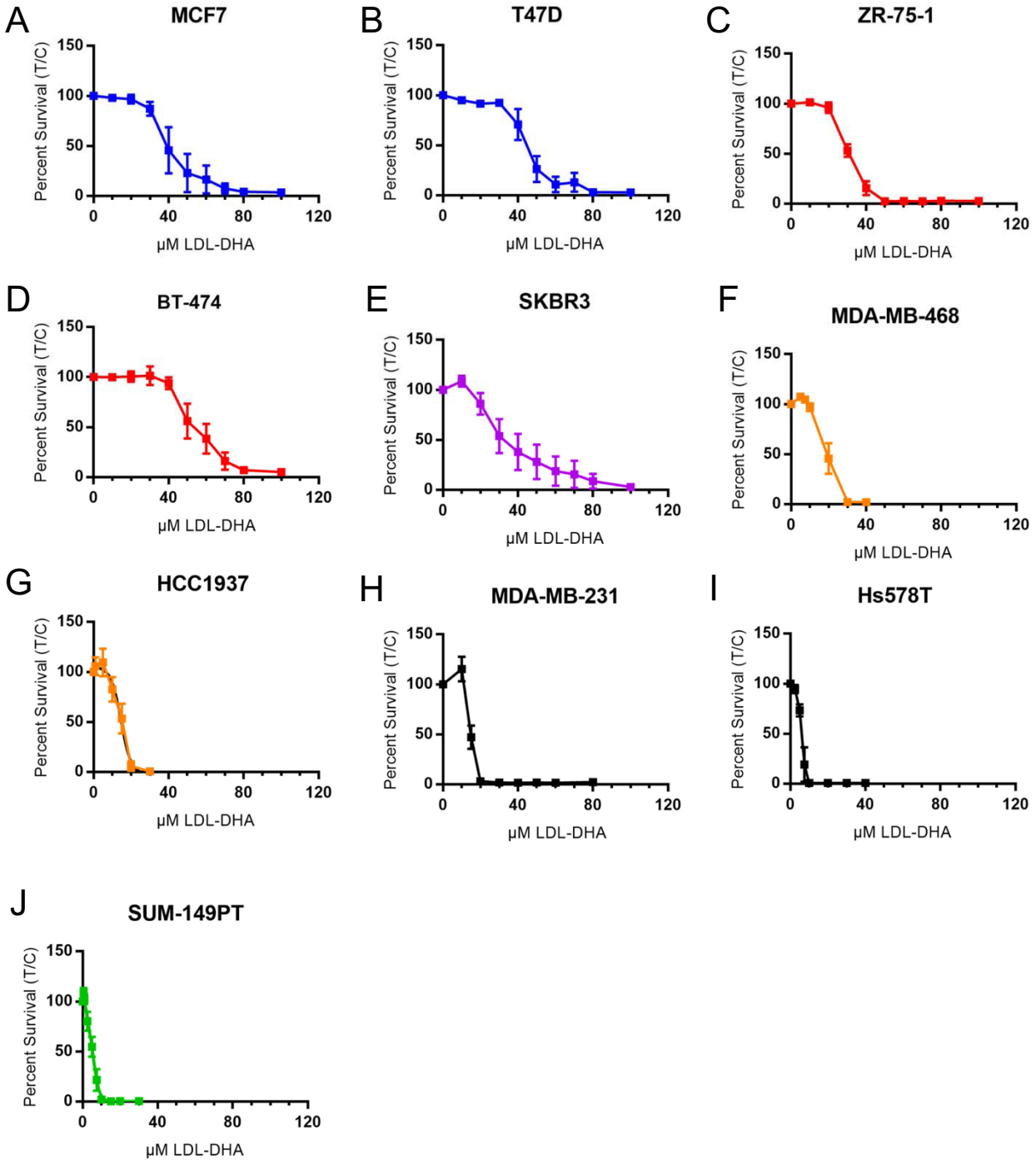

Figure 1 Cytotoxicity of LDL-DHA in breast cancer cells. Cells were treated with LDL-DHA nanoparticles under serum starve conditions for 72 hours with a dose range of 0–100uM for hormone responsive cell lines (Luminal A (Blue) Luminal B (Red) HER2 Enriched (Purple)) and 0–40 or 80uM for triple negative cell lines (Basal Like (Orange) Claudin Low (Black) and Inflammatory (Green)). Dose response is shown for each cell line in (**A**) MCF7, (**B**) T47D, (**C**) ZR-75-1, (**D**) BT-474, (**E**) SKBR3 (**F**) MDA-MB-468 (**G**) HCC1937 (**H**) MDA-MB-231 (**I**) Hs578T and (**J**) SUM-149PT.

cells express wild-type LDLR and SR-B1, ldlA7 has mutant inactive LDLR and wild-type SR-B1, and ldlA7[mSR-B1] has mutant inactive LDLR and overexpression of murine SR-B1 (Figure 2E). Upon treating these cells with LDL-DiI-OA , we found that the DiI signal associated with the ldlA7[mSR-B1] cells significantly increased in a dose-dependent manner (Figure 2E). In contrast, the DiI signal associated with CHO-K1 and ldlA7 cells was much lower in magnitude

https://doi.org/10.2147/BCTT.S554396

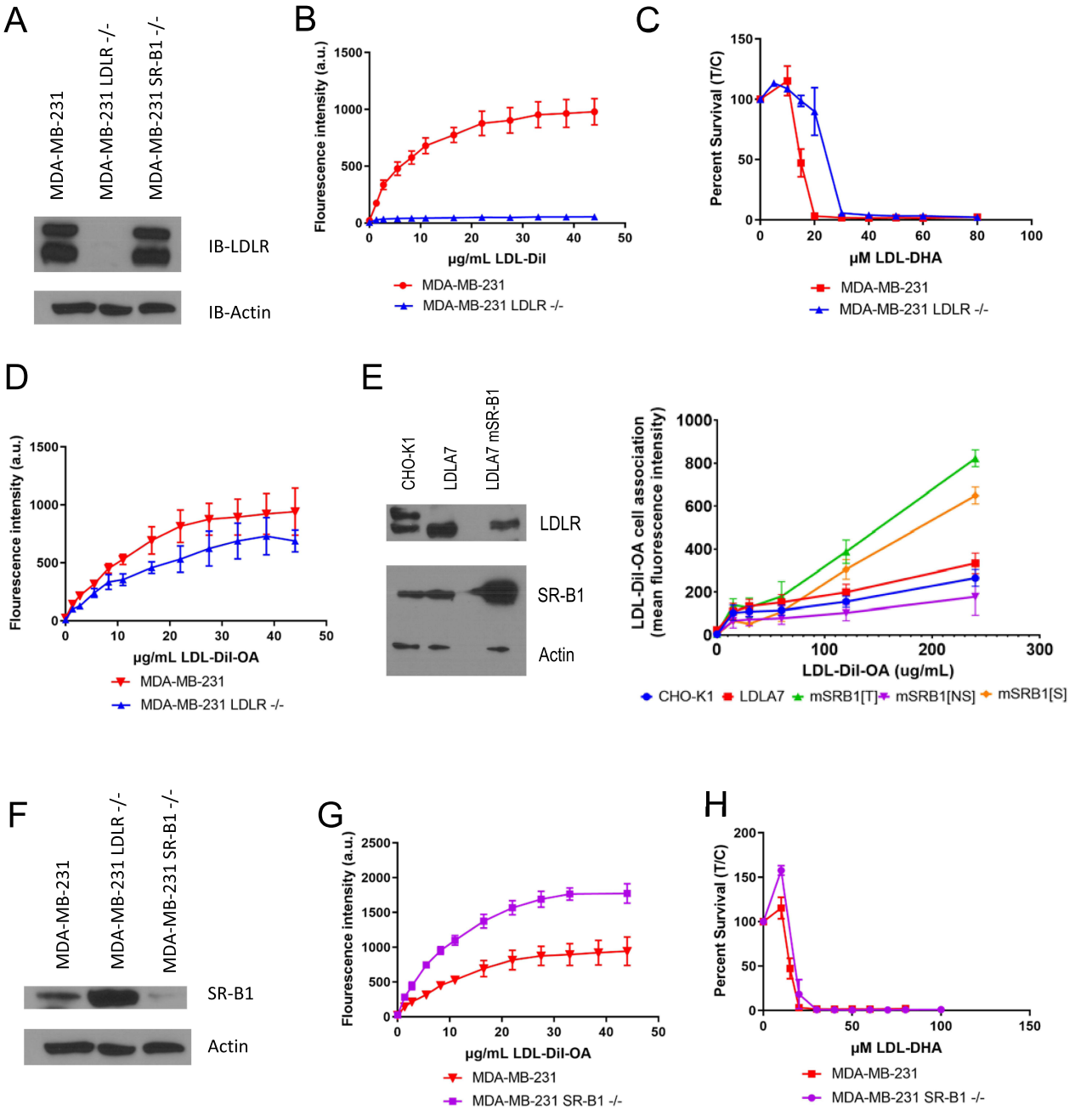

Figure 2 Single knockouts of LDLR and SR-B1 are unable to protect from LDL-DHA treatment. (**A**) Western blot showing LDLR expression in wild type, LDLR and SR-B1 knockout MDA-MB-231s under normal growth conditions. Actin was used as a loading control. (**B**) LDL-DiI association in wild type MDA-MB-231 and LDLR knockout MDA-MB-231s. Association was done under serum starve conditions with a 6-hour treatment of LDL-DiI, cells were then harvested, and uptake was measured by FACS. (**C**) Dose response to LDL-DHA nanoparticles in wild type and knockout MDA-MB-231s. Cells were treated with increasing doses of LDL-DHA (10–100µM) for 72 hours under serum starve conditions. (**D**) LDL-DiI-OA uptake in wild type and LDLR deficient MDA-MB-231 cell lines. Cells were treated with increasing doses of LDL-DiI-OA for 6 hours under serum starve conditions. Fluorescence intensity of DiI was then measured by FACS. (**E**) LDLR and SR-B1 expression by Western blot in CHO-K1, LDLA7 and LDLA7-mSRB1 cells. LDL-DiI-OA uptake in CHO-K1, LDLA7 and LDLA7-mSRB1 cells. Cells were serum starved overnight followed by treatment with LDL-DiI-OA for 2 hours at 37C. The cells were then collected and mean fluorescence intensity quantified using FACS. For excess HDL group, the cells were pre-treated for 30 min with 40-fold excess HDL. The ldlmSR-B1[S] (specific value, Orange trace) represents the difference between ldlmSR-B1[T], total (green trace) and ldlmSR-B1[NS], nonspecific (purple trace) (40-fold excess unlabeled HDL). (**F**) SR-B1 expression by Western blot in wild type, LDLR and SR-B1 knockout MDA-MB-231s under normal growth conditions. Actin is used as a loading control. (**G**) LDL-DiI-OA Uptake in SR-B1 knockout and wild type MDA-MB-231 cells. This was done under serum starve conditions followed by 6-hour treatment with increasing doses of LDL-DiI-OA followed by FACS. (**H**) Dose Response to LDL-DHA in SR-B1 knockout and wild type MDA-MB-231s under serum starve conditions with a dose range of 10–100µM for 72 hours. Data is expressed as mean ± SEM. Western Blot Molecular weights: LDLR (Upper 140 kD, Lower 92 kD); SR-B1 (82kD); and actin (42 kD).

and displayed more saturable kinetics (Figure 2E). Given that LDLR is defective in ldlA7 and ldlA7[SR-B1], these results indicate that SR-B1 is capable of binding and transporting LDL-DiI-OA nanoparticles.

We next generated SR-B1 CRISPR knockout MDA-MB-231 cells (MDA-MB-231 SR-B1-/-), which retained LDLR expression at similar levels to wild-type cells (Figure 2A and F), and proceeded to evaluate the uptake of LDL-DiI-OA nanoparticles. Surprisingly, the uptake of LDL-DiI-OA in the MDA-MB-231 SR-B1-/- cells exceeded that seen in the wild-type MDA-MB-231 cells (Figure 2G). The LDL-DHA dose response curves were equivalent between MDA-MB -231 SR-B1-/- and their wild type counterparts (Figure 2H). We also created a knockdown for CD36 (another member of the scavenger receptor family) and found that it had a small effect on uptake and slight protection from LDL-DHA cytotoxicity (Supplementary Figure 2). Collectively, these findings suggest that while LDL-DHA nanoparticles can enter the cell by SR-B1, LDLR interactions/endocytosis are preferred.

LDL-DiI-OA Uptake Across Breast Cancer Cell Panel

Upon establishing that LDL-DHA enters cells primarily through LDLR and SR-B1, we turned back to our panel of breast cancer cells to evaluate LDL-DiI-OA uptake. Figure 3 shows the uptake of LDL-DiI-OA nanoparticles for MCF7 (3A), T47D (3B), ZR-75-1 (3C), BT-474 (3D), SKBR3 (3E), MDA-MB-468 (3F), HCC1937 (3G), MDA-MB-231 (3H), Hs578T (3I) and SUM-149PT (3J). Calculated Kd and Bmax values for each cell line are shown in Supplementary Table 2. The data from these experiments represent the total association of LDL-DiI-OA with the breast cancer cell, thus reflecting processes of binding, internalization, and degradation over the multiple courses of receptor recycling to the cell surface. Thus, we interpret Bmax as the maximum amount of internalization and receptor binding these cells have, and it is a reflection of how much LDL-DHA would be delivered to the cell at a comparable dose. Kd reflects the dose at which the processes of receptor binding, internalization, and any receptor recycling are half-saturated. Bmax values were higher for triple-negative cell lines, indicating higher uptake and internalization of LDL-DiI-OA in these cells. Kd Values were far more heterogeneous, as this reflects many different processes that are involved.

To decipher the contributions of LDLR and SR-B1 on the binding and uptake of LDL nanoparticles in each breast cancer cell, we performed assays to determine the capacity of LDL or HDL to block LDL-DiI-OA association. This was done by treating cells with LDL-DiI-OA at 10 ug protein per mL and then treating with a 20-fold protein excess of LDL, HDL, or a combination of 20-fold excess of LDL and 20-fold excess of HDL. Figure 4 shows the response to excess LDL and HDL for MCF7 (4A), T47D (4B), ZR-75-1 (4C), BT-474 (4D), SKBR3 (4E), MDA-MB-468 (4F), HCC1937 (4G), MDA-MB-231 (4H), Hs578T (4I), SUM-149PT (4J) MDA-MB-231 LDLR -/- (4K) and MDA-MB-231 SR-B1-/- (4L). Excess LDL was able to effectively inhibit the association of LDL-DiI-OA across all breast cancer subtypes. Meanwhile, excess HDL showed equivalent levels of inhibition among most of the Luminal A and B subtypes (MCF7, ZR-75-1 and BT-474) and Basal-like cell line Hs578T. Moderate levels of excess HDL inhibition were detected in SKBR3, MDA-MB-468 and MDA-MB-231. The capacity for excess HDL to inhibit LDL-DiI-OA association was least for T47D, HCC1937 and SUM-149T. Finally, the association of LDL-DiI-OA among the knock-out MDA-MB-231 LDLR-/- and SR-B1-/- was predominantly inhibited by excess HDL and LDL, respectively.

We then looked at receptor expression in all of these cell lines (Figure 5). Relatively high levels of LDLR expression were seen in the luminal A (MCF7 and T47D); hormone-sensitive SKBR3; and the basal, MDA-MB-468, HCC1937, and MDA-MB-231. SR-B1 expression was high among Luminal A (MCF7 and T47D), Luminal B (ZR-75-1), Hormone-sensitive SK-BR3, and the Basal-like cell-line Hs578T. We noticed here a reciprocal relationship where cells that have high expression of LDLR have lower expression of SR-B1. Triple negative cell lines for the most part favor high LDLR expression and hormone responsive lines presenting accompanying high SR-B1 expression.

Confocal Microscopy Highlights Differences in LDLR and SR-B1 Dependent Uptake

LDLR and SR-B1 have distinct interactions with lipoproteins which involve receptor-mediated endocytosis and select lipid transfer, respectively.[59,60] Both of these internalization processes can be visualized with cellular imaging methods. Confocal microscopy was employed with wild-type MDA-MB-231 cells to document the uptake of LDL-DiI (LDLR-mediated endocytosis), HDL-DiI (SR-B1-mediated lipid transfer) and LDL-DiI-OA (combined endocytosis and select

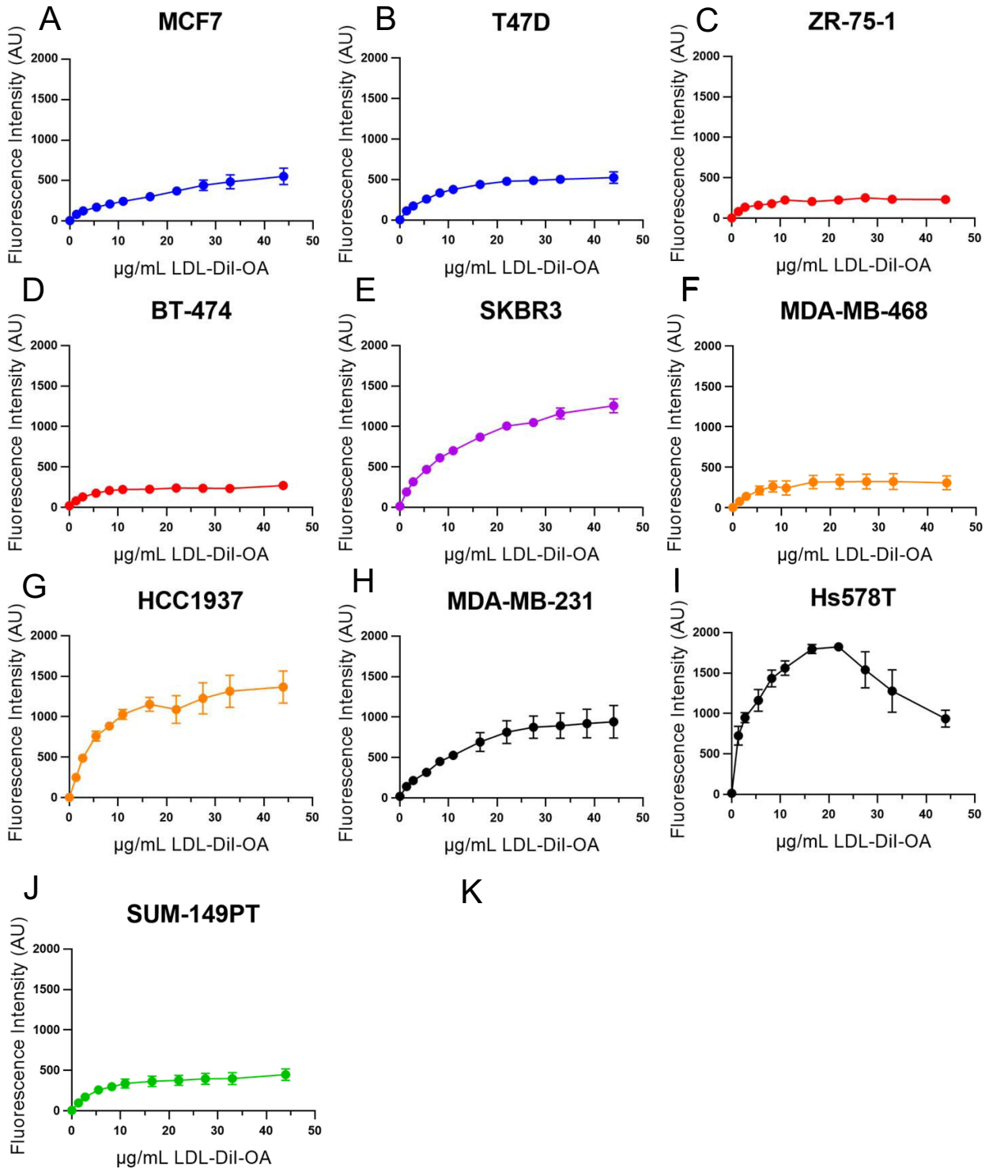

Figure 3 LDL-DiI-OA uptake across breast cancer cell panel. LDL-DiI-OA uptake. Cells were treated with increasing doses of LDL-DiI-OA for 6 hours under serum starve conditions. Fluorescence intensity of DiI was then measured by FACS. LDL-DiI-OA is representative of LDL-DHA uptake. Response is shown for each cell line in (**A**) MCF7, (**B**) T47D, (**C**) ZR-75-1, (**D**) BT-474, (**E**) SKBR3 (**F**) MDA-MB-468 (**G**) HCC1937 (**H**) MDA-MB-231 (**I**) Hs578T and (**J**) SUM-149PT.

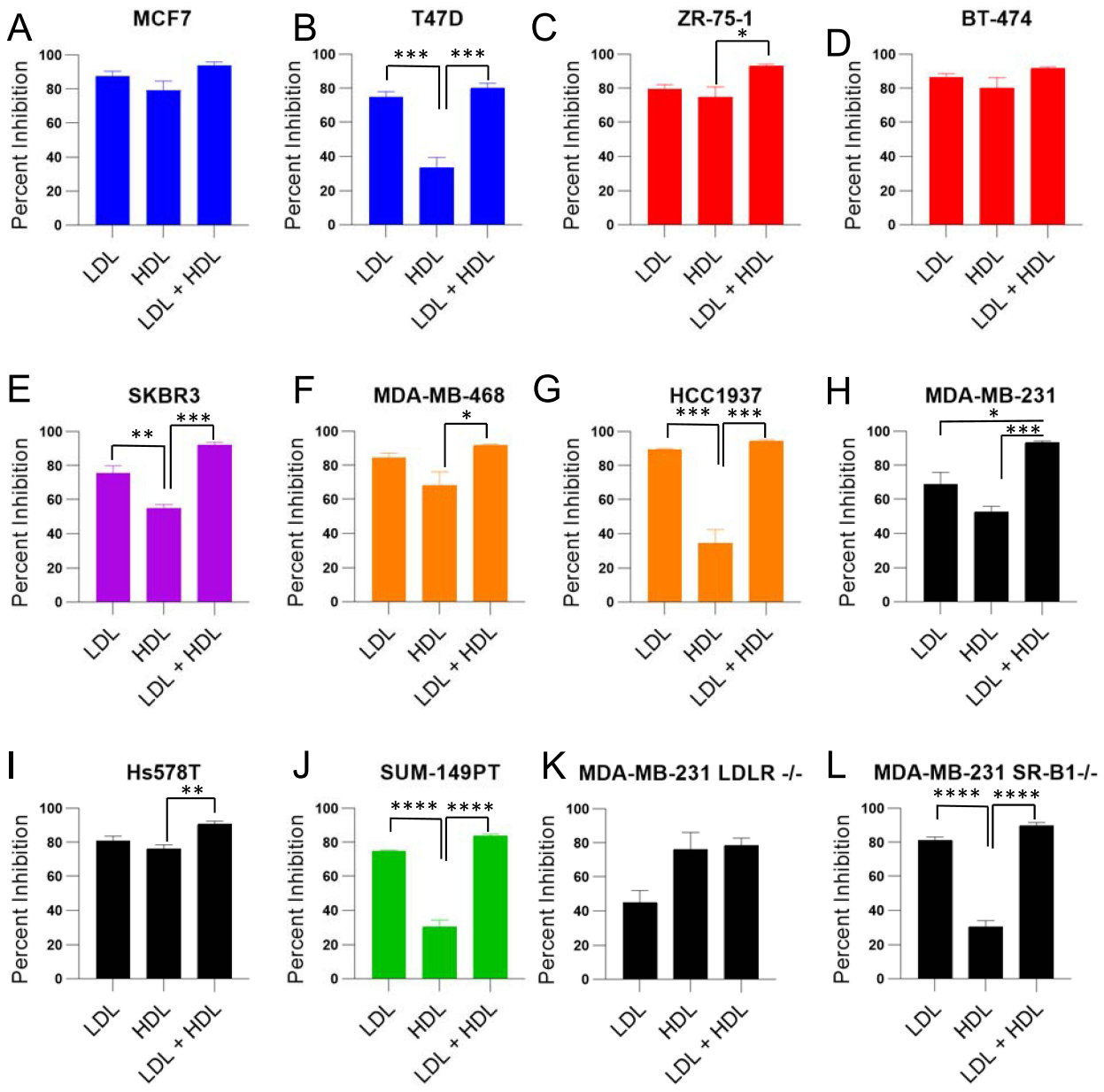

Figure 4 Inhibition of LDL-DiI-OA with excess LDL and HDL show the balance between LDL and SR-B1. The panel of Breast cancer cells were pre-treated under serum starve conditions with either 200ug LDL 200ug HDL or 200ug LDL+ 200ug HDL, after 1Hr cells were treated with 10ug of LDL-DiI-OA for 6 hours. Fluorescence intensity of DiI was then measured by FACS. Control treatment was done concurrently to normalize data to percentage by dividing total inhibited uptake by control uptake then subtracted from 100% to show total inhibition by treatment condition, each panel show the inhibition plot for each cell with each cell line in the following panels (**A**) MCF7, (**B**) T47D, (**C**) ZR-75-1, (**D**) BT-474, (**E**) SKBR3 (**F**) MDA-MB-468 (**G**) HCC1937 (**H**) MDA-MB-231 (**I**) Hs578T (**J**) SUM-149PT (**K**) MDA-MB-231 LDL-/- and (**L**) MDA-MB -231 SR-B1-/-. Data is expressed as mean ± SEM. *, P<0.05; **, P<0.01; ***, P<0.001 and ****, P<0.0001.

lipid transfer) (Figure 6). The cell-permeable dye LysoSensor was used to stains the lysosomes and co-register the DiI for receptor-mediated endocytosis.

Our MDA-MB-231 knock-out cells were also investigated with confocal microscopy to demonstrate distinct uptake patterns related to receptor-mediated endocytosis in SR-B1-/- and selective lipid transfer in LDLR-/- (Figure 6). Microscopy studies with LDL-DiI-OA were also extended to SKBr3 and ZR-75-1 cells, which showed the fluorescence signal to be LDLR dominant in SK-BR3, while ZR-75-1 showed a more SR-B1 dominant pattern (Figure 6).

https://doi.org/10.2147/BCTT.S554396

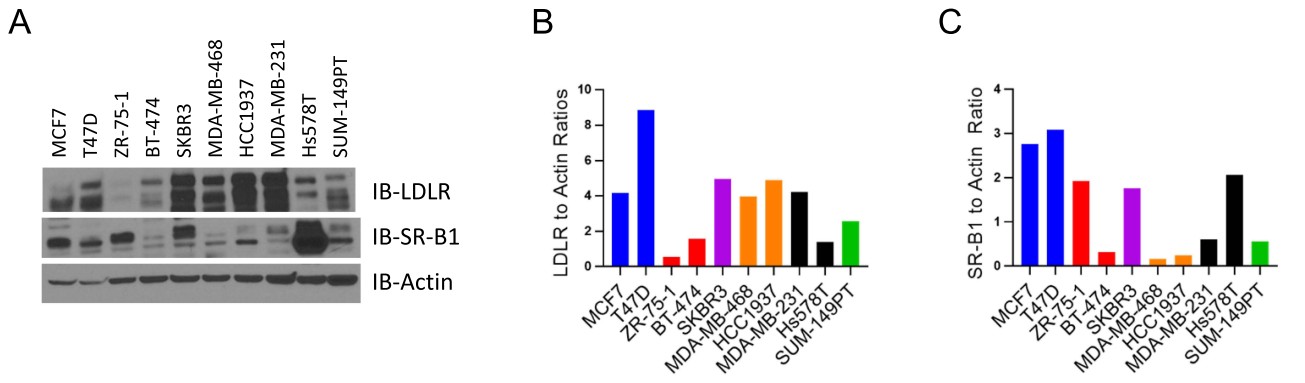

Figure 5 Protein expression of LDLR and SR-B1. (**A**) Western blot of LDLR and SR-B1 receptor expression in panel of breast cancer cells under normal growth conditions. Actin was used as a loading control. (**B**) Quantification of LDLR to Actin ratio and (**C**) SR-B1 to Actin ratio. Western Blot Molecular weights: LDLR (Upper 140 kD, Lower 92 kD); SR-B1 (82kD); and actin (42 kD).

Dual Blockade of LDLR and SR-B1 Diminishes LDL Nanoparticle Uptake and Cytotoxicity

Concurrent inhibition of LDLR and SR-B1 was achieved by pharmacologic and genetic methods. In the former, association experiments were carried out with wild-type MDA-MB-231 and MDA-MB-231 LDLR-/- cells, where LDL-DiI-OA was incubated in the presence or absence of an antibody directed to the extracellular domain of SR-B1 (Figure 7A). The LDLR-/- alone showed a 40–50% reduction in LDL-DiI-OA association/uptake compared to wild-type cells. The addition of the SR-B1 antibody to the LDLR-/- cells resulted in a further 50% reduction in LDL-DiI-OA association/uptake. SR-B1 antibody antagonism had little to no effect on the uptake/association of LDL-DiI-OA in wild-type MDA-MB-231 cells.

Next, we utilize suramin, a high-affinity polysulfonated naphthylurea known to bind to LDL particles and block receptor interactions. We found that suramin was able to ablate association/uptake in all cell lines to near zero (Supplementary Figure 3).

To establish a dual LDLR and SR-B1 knockout line, our MDA-MB-231 LDLR-/- line was treated with a shRNA for SR-B1 to create our MDA-MB-231 LDLR-/- shSR-B1 line (Figure 7B). Association curves showed wild-type MDA-MB -231 cells to have the highest association, followed by MDA-MB-231 LDLR-/- cells showing an approximate 25% reduction from wild type, and finally, the MDA-MB-231 LDLR-/-shSR-B1 cells showed the least uptake/association. At the highest LDL-DiI-OA concentration (45 μg/mL) the uptake/association in the MDA-MB-231 LDLR-/- shSR-B1 was less than 50% of that seen in wild-type cells (Figure 7C). Confocal imaging of LDL-DiI-OA association in MDA-MB -231 LDLR-/-shSR-B1 showed minimal fluorescent uptake (Figure 7D).

Cell viability experiments were then performed with LDL-DHA in a pulse-chase format with wild-type, LDLR-/-, shSR-B1, and LDLR-/- shSR-B1 MDA-MB-231 cells with 25uM LDL-DHA for 1, 3, 6, and 24 hours. The LDL-DHA-containing media were replaced with fresh media at these time points, then viability was measured at 24-hours post-treatment (Figure 7E). From the 1-hour exposure, the LDL-DHA reduced the viability of the wild-type MDA-MB-231 cells to 25%, however each of the single and double knock out cells were able to preserve viability in excess of 70%. From the 3, 6 and 24 hour exposures step-wise increasing protection was seen with LDLR-/-, shSR-B1 and LDLR-/- shSR-B1 genetic constructs. At 6 and 24 hour exposures LDL-DHA cytotoxicity achieved almost complete kill of wild-type MDA-MB-231 cells, meanwhile, the MDA-MB-231 LDLR-/- shSR-B1 cells were able to stave off this assault, maintaining cell viability near 50%. These findings indicate that LDLR and SR-B1 play a predominant role in facilitating the uptake and subsequently eliciting cytotoxicity of LDL-DHA nanoparticles in breast cancer cells.

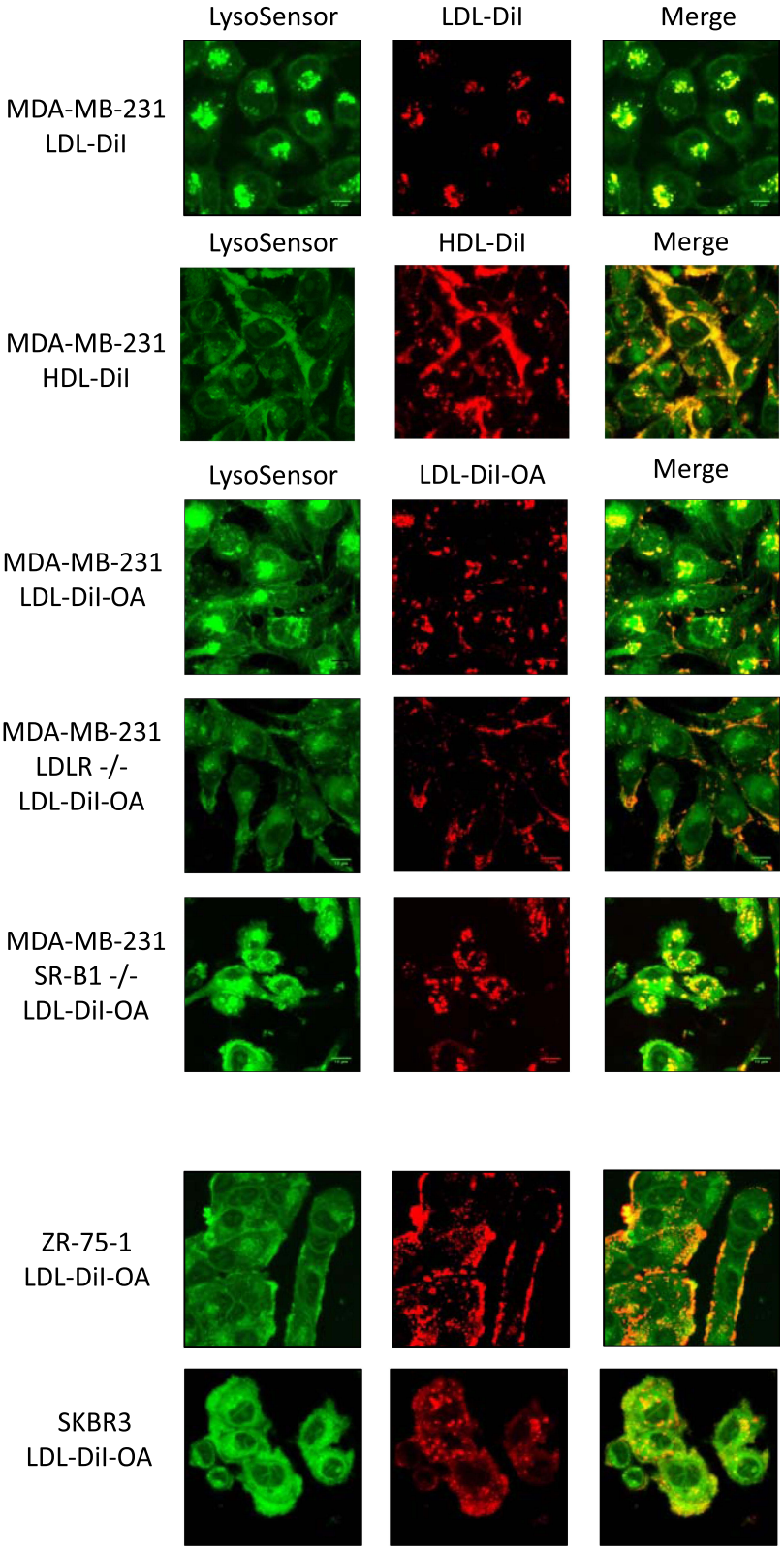

Figure 6 Confocal microscopy of LDL-DiI, HDL-DiI, and LDL-DiI-OA uptake. LDL-DiI and HDL-DiI in MDA-MB-231s is shown to highlight LDLR-mediated endocytosis (LDL-DiI) and SR-B1-mediated selective lipid uptake (HDL-DiI). LDL-DiI-OA is shown in Wild Type, LDLR-/-, and shSR-B1 MDA-MB-231 cells, showing how each uptake pathway is perturbed by these knockouts. LDL-DiI-OA treatment in SKBr3 and ZR-75-1 cells shows respective LDLR-dominant and SR-B1 dominant uptake patterns. Cell type and treatment are listed on the left.

https://doi.org/10.2147/BCTT.S554396

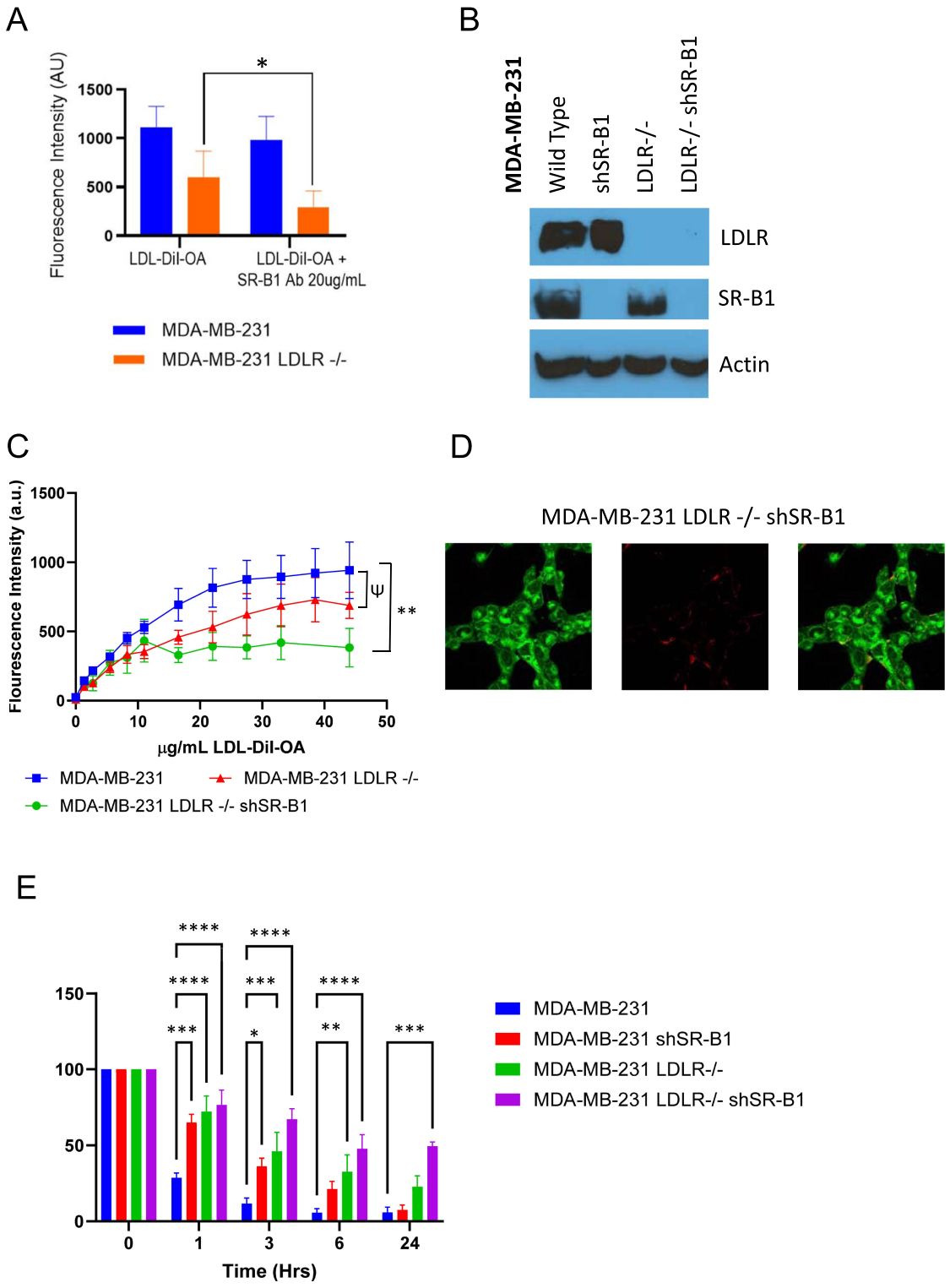

Figure 7 Use of double knockout of LDLR and SR-B1 shows some rescue to LDL-DHA treatment. (**A**) Use of an SR-B1 antibody to inhibit LDL-Dil-OA Uptake in wild-type LDLR Knockout MDA-MB-231s. Cells were treated under serum-starved conditions, then were given a 1-hour pretreatment of an SR-B1 antibody or mock antibody treatment. Continued cotreatment with LDL-Dil-OA was then performed for 6 hours. Cells were then harvested, and Dil fluorescence was measured by FACS. Data is expressed as mean ± SEM. Statistical analysis was done by a paired Student's *T*-test with pairs comprising of same cell experimental replicates. (**B**) Protein expression of LDLR and SR-B1 in Wild Type, LDLR-/-, shSR-B1, and LDLR-/- shSR-B1 MDA-MB-231 cells. (**C**) LDL-Dil-OA uptake in MDA-MB-231, LDLR-/- and LDLR-/- shSR-B1. (**D**) Confocal image of MDA-MB-231 LDLR-/- -shSR-B1 cells 2 hours following incubation with LDL-Dil-OA. (**E**) Dose response to a 1-, 3-, 6-, and 24-hour pulse of LDL-DHA. After each pulse (with the exception of 24 hours) the media was changed, and the cell viability was read out at 24 hours. Data is expressed as mean ± SEM. Ψ, P= 0.06, *, P<0.05; **, P<0.01; ***, P<0.001 and ****, P<0.0001. Western Blot Molecular weights: LDLR (Upper 140 kD, Lower 92 kD); SR-B1 (82kD); and actin (42 kD).

Role of Potential Other Receptors

The regulation of cholesterol homeostasis was investigated in MDA-MB-231 cells and their knockout variants by qPCR. Twelve regulatory genes encompassing: master transcription factors (SBREP-1a and SRBEP-1c); cholesterol biosynthesis genes (Fpp Synthase, HMG COA Reductase, HMG COA Synthase, INsig-1 and Squalene synthase); and cholesterol transport/internalization (ALK-1, CD36, LDLR and LOX-1) Supplementary Figures 4 and 5. We observed that overnight fasting (performed before LDL nanoparticle treatments) resulted in increased LDLR expression, an increase in the cholesterol biosynthesis genes and an increase in SREBP-1c. We were also able to further validate the expression of our knockouts of LDLR and SR-B1. Single LDLR knock out and dual LDLR and SR-B1 knockouts induced an increase in ALK-1, CD36, cholesterol biosynthesis, and SREBP-1c genes. It should be noted that in wild-type MDA-MB-231, the expression of the alternate transport/internalization genes CD36, LOX-1, and ALK-1 are expressed at a significantly (> 100-fold less) lower level when compared to the expression of LDLR.

Antagonizing Cholesterol Biosynthesis Enhances LDL-DHA Cytotoxicity

Given the obligatory need for breast cancer cells to increase their cholesterol pools either through cholesterol biosynthesis or uptake, we explored whether blocking cholesterol biosynthesis would enhance LDL-DHA nanoparticle acquisition and cytotoxicity. For these experiments, MCF7 and MDA-MB-231 cells were treated with a combination of simvastatin (an HMG-CoA reductase inhibitor) and LDL-DHA, and cytotoxicity was assessed 24 hours later (Figure 8). This combination treatment demonstrated an additive effect between LDL-DHA and Simvastatin in both MCF7 and MDB-MB-231 cells.

Lipid Peroxidation Response Varies Across Breast Cancer Cells Following LDL-DHA Treatment

Lipid peroxidation is a common sequelae following LDL-DHA uptake in cancer cells. Examination across select cells of our breast cancer panel (MCF7, ZR-75-1, SKBr3, HCC1937, MDA-MB-231, and SUM-149PT) revealed varied responses (Figure 9). The levels of lipid peroxidation actually decreased in MCF7 cells with increasing concentrations of LDL-DHA treatment (Figure 9A). In the MDA-MB-231 cells, lipid peroxidation levels remained unchanged across the treatment doses of LDL-DHA (Figure 9E). For the other cell lines we tested, lipid peroxidation levels approached 2-fold for ZR-75-1, 3-fold for SUM-149PT, 4-fold for SKBR3, and nearly 15-fold for HCC1937. Combined, these findings suggest altered lipid metabolism across our breast cancer panel.

To elucidate the mechanisms governing the different lipid peroxidation responses to LDL-DHA treatment, PCR analysis was performed on a panel of antioxidant genes (Supplementary Figure 6). For this study, representative responses of enhanced, unchanged, and decreased lipid peroxidation were evaluated in HCC1937, MDA-MB-231, and MCF7, respectively. The dose-dependent diminution of lipid peroxidation activity in MCF7 was consistent with the relatively high expression of glutathione synthesis (glutamate-cysteine ligase (GCLC)) and reducing capacity (glutathione peroxidase 4 (GPX4)), peroxiredoxins (PRDX1 and 6), and superoxide dismutase (SOD1 and SOD2). MDA-MB-231 cells expressed moderate levels of all antioxidants and the greatest levels of the cystine/glutamate transporter (SLC7A11), which facilitates in subduing any increases in lipid peroxidation following LDL-DHA treatment. Conversely, HCC1937 expressed minimal levels of all the antioxidant genes (GCLC, GPX4, PRDX6, SLC7A11, SOD1, and SOD2), thus leaving it susceptible to LDL-DHA-induced lipid peroxidation.

LDL-DHA Mediates Apoptosis Cell Death in Breast Cancer Cells

Cell death measurements were performed by Annexin V/propidium iodide staining on a select group of cells from our breast cancer panel. With the exception of SKBR3, all other cells showed evidence of both apoptosis and necrosis processes occurring after LDL-DHA treatment (Figure 9G–L). In this assay, SKBR3 displayed a predominance of necrotic cell death. Secondary measures of apoptosis were followed up employing a luminescence-based specific caspase activity assay (Supplementary Figure 7). The cell lines HCC1937, MDA-MB-231, MCF7, Sum-149PT, and ZR-75-1 all demonstrated a significant induction of caspase activity with LDL-DHA treatment. Interestingly, SKBR3 also showed increased activity.

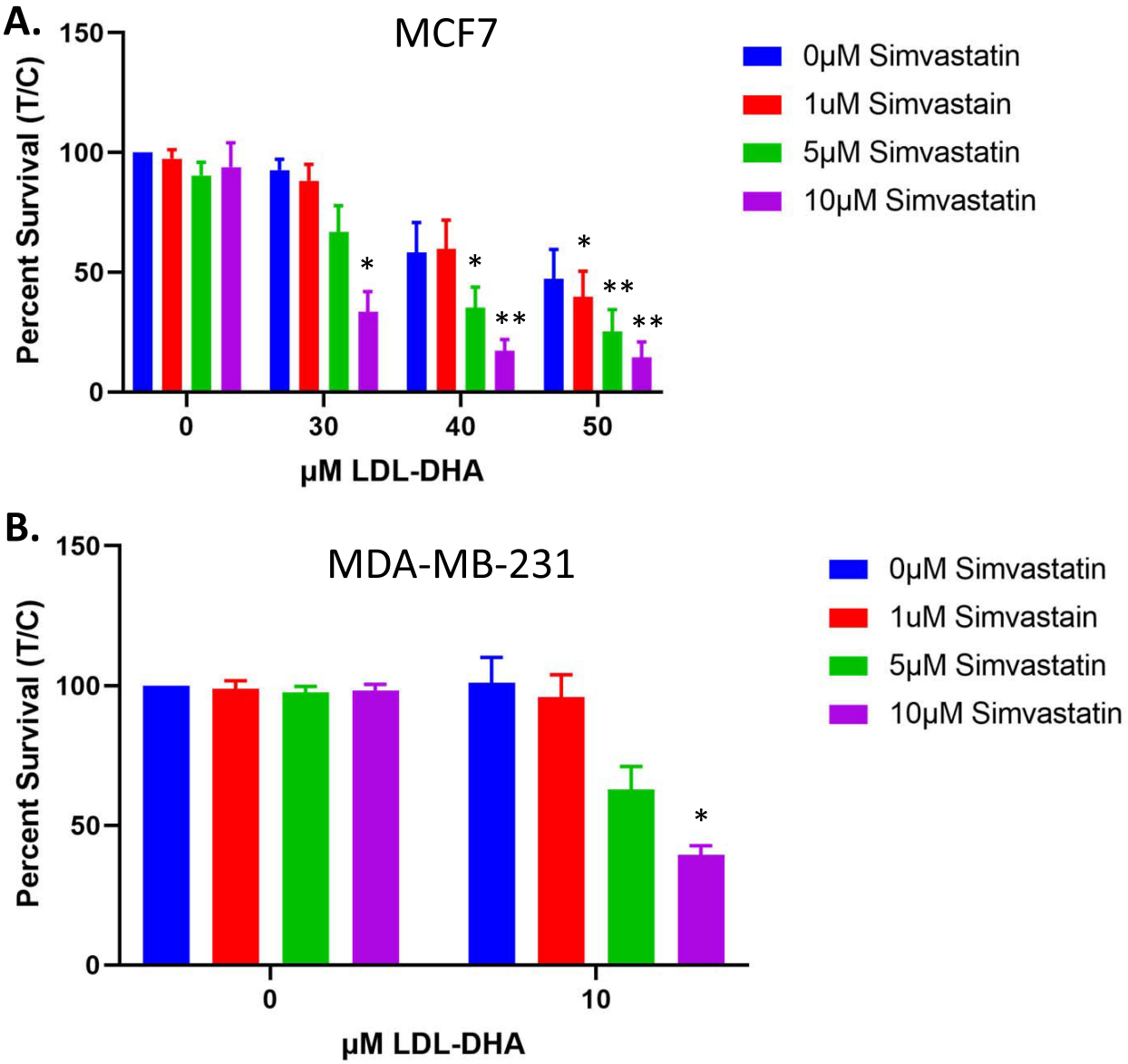

Figure 8 Co-treatment of LDL-DHA and simvastatin in MCF7 (**A**) and MDA-MB-231 (**B**). MCF7 and MDA-MB-231 cells were pre-treated under serum starve conditions with indicated doses of simvastatin for 1hour followed by 24 hour co-treatment with LDL-DHA. Viability was read out at 25 hours post simvastatin treatment. Data is expressed as mean ± SEM. *, P<0.05; **, P<0.01 compared to equivalent simvastatin counterpart without LDL-DHA treatment.

Discussion

Breast cancer cells exhibit a voracious appetite for lipids, in particular cholesterol. In general, cells meet this need through biosynthetic and uptake processes. It has been observed that tumors with higher expression of HMG-CoA reductase tend to be less aggressive (smaller tumor size, low histological grade, low Ki67 index, high p27 expression), displaying prognostically favorable tumor parameters compared to tumors with low HMG-CoA reductase.[25] Conversely, tumors that rely on sequestering cholesterol from their environment (ie, tumors with high expression of LDLR) tend to have accelerated tumor growth and be associated with the triple negative phenotype.[37,61] Furthermore, patients with these tumors tend to have shorter recurrence-free survival and poorer prognosis overall. This has led various groups to consider leveraging the natural ability of LDL to target breast and other tumor types.[62–64] Indeed, several groups have functionalized the LDL platform with numerous diagnostic and therapeutic agents. While this strategy can provide tumor

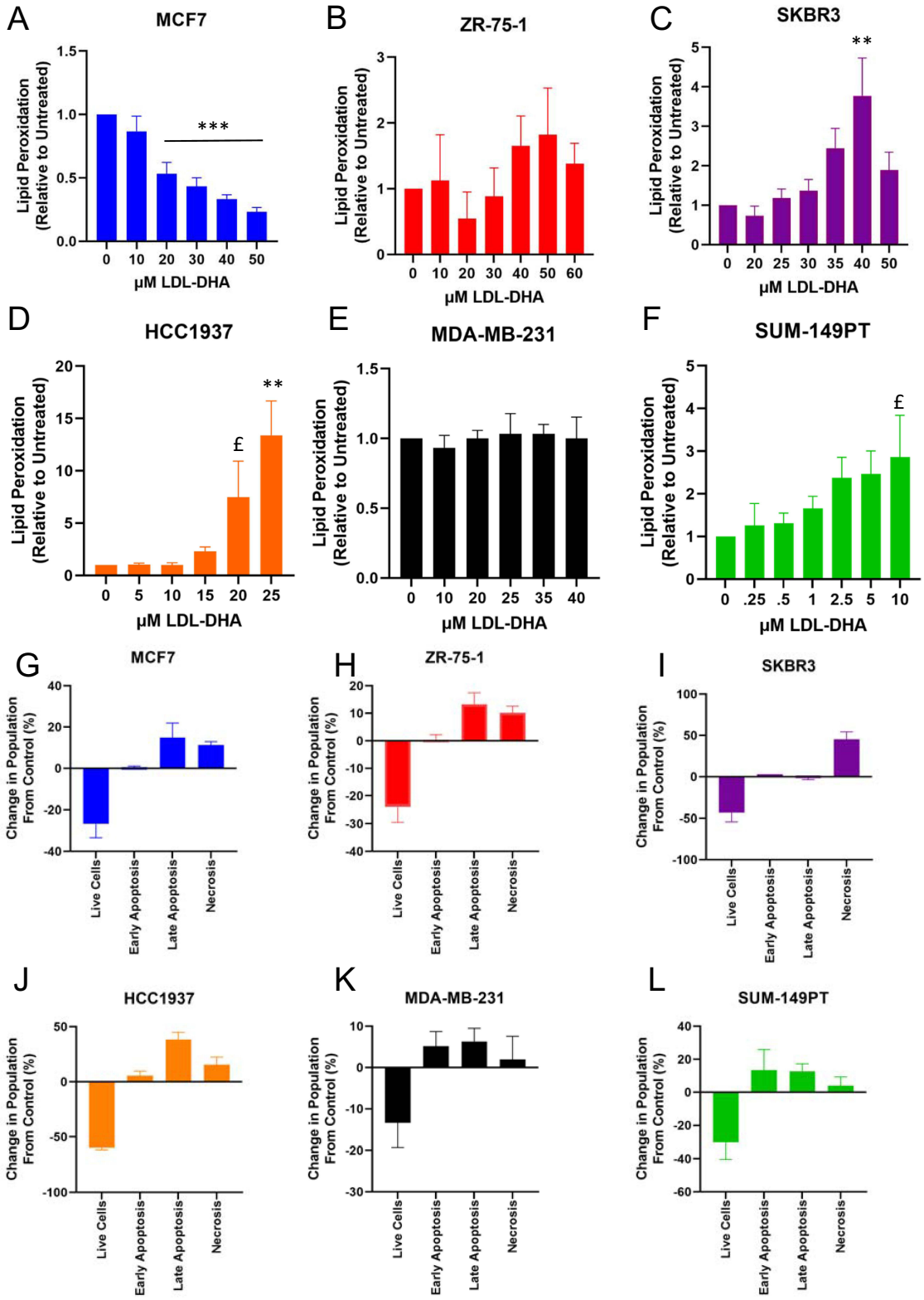

Figure 9 Lipid peroxidation and Annexin V/PI apoptosis assay analysis shows induction of lipid peroxidation in breast cancer cells. (**A**–**F**) Lipid Peroxidation by FACS using Bodipy C11 in (**A**) MCF7, (**B**) ZR-75-1, (**C**) SKBR3, (**D**) HCC1937, (**E**) MDA-MB-231, (**F**) SUM-149PT. (**G**–**L**) Induction of apoptosis shown as change in percentage representation for each category from untreated controls in (**G**) MCF7, (**H**) ZR-75-1, (**I**) SKBR3, (**J**) HCC1937, (**K**) MDA-MB-231s, (**L**) SUM-149PT. Data is expressed as mean ± SEM. *, P<0.05; **, P<0.01; ***, P<0.001 compared to non-treated control.

https://doi.org/10.2147/BCTT.S554396

targeting, however, caution must be taken as most, if not all, cells express LDLR. As such, utilization of the LDL-based drug delivery approach would require the use of cancer-selective cytotoxic agents. While many investigators have formulated conventional chemotherapeutic drugs into the LDL platform, few have advanced beyond in vitro cell experiments or limited small animal studies. Caveats that hinder this approach include restricted drug payloads and compromised carrier-drug stability. Low drug encapsulation (in the order of 10s to 100s drug molecules per LDL) and rapid drug-plasma protein associations markedly detract from the LDL drug delivery concept.[65]

Docosahexaenoic acid, a natural long-chain polyunsaturated fatty acid, has been implicated in reduced cancer risk for a number of tumor types. Favorable outcomes have been reported in large prospective cohort studies of breast cancer patients, where individuals with the highest intake of omega-3 PUFAs experienced a reduction in breast cancer risk compared to those with low intake of marine PUFAs.[66] Intake of DHA/EPA is also associated with improvements in survivorship after breast cancer diagnosis, reductions in breast cancer recurrence (25%), and improved overall mortality have been reported.[67] More recently, studies by Bobin-Dubigeon et al highlighted that the association of circulating EPA/DHA with apoB-containing lipoproteins correlated with reduced tumor proliferation among patients with hormone receptor-negative breast cancer.[68] These seminal findings further validate the anticancer strategy our group has established in re-engineering plasma LDL to transport DHA. The engineered LDL-DHA construct retains nanoscale dimensions (~22 nm in diameter) while incorporating 1500–2000 molecules of DHA.[53] The molecular organization of LDL-DHA, unlike plasma LDL, entails a phospholipid bilayer, net electronegative surface charge, and thermodynamic and kinetic stabilities that surpass those of native LDL.[51] The conformation of the apoB-100 protein is retained in this structure, allowing the particle to readily interact with LDLR.[53] Halo-particle uptake and subsequent trafficking through endo-lysosomal pathways have also been documented for this particle.[69] Indeed, many other groups have attempted to target the overexpression of LDLR in their efforts to deliver anticancer agents to tumors.[70] The purview of relying on LDLR overexpression is somewhat limiting, given that tumors may express equivalent or even lower levels of LDLR compared to surrounding steroidogenic tissues.

Findings in the present study indicate that LDL-DHA nanoparticles surpass native LDL in its capacity to interact with cell surface receptors beyond LDLR, namely SR-B1, better known as the HDL receptor. Evidence for this binding is supported by the uptake studies of LDL nanoparticles in LDLR knock-out MDA-MB-231 and ldlA7[mSR-B1] cells. Unlike LDLR, SR-B1 mediates the selective uptake of lipids from lipoproteins, where lipids are transferred to the cell without internalization of the intact lipoprotein.[71] The LDL nanoparticles demonstrated significantly greater binding and lipid transfer via SR-B1 than could be seen with native LDL. The enhanced interactions between LDL nanoparticles and SR-B1 may be explained by the net electronegative surface charge of LDL nanoparticles, as SR-B1 is a multi-ligand receptor known to have a high affinity for anionic phospholipids.[72] Confocal imaging demonstrated a clear pattern of SR-B1-mediated lipid uptake as LDL-DiI-OA fluorescence was observed throughout the cell membrane with little lysosomal co-localization. Our studies also demonstrated the compensatory cellular mechanisms for cholesterol uptake; in response to LDLR knock out, SR-B1 expression was upregulated. Other groups have also noted compensatory responses among lipoprotein receptors.[73] Given cancer cells' obligatory need for cholesterol, mechanisms are activated to ensure ample levels of intracellular cholesterol are available. Given this line of reasoning, the combination of LDL-DHA with a statin (Simvastatin) may prove to be an attractive therapeutic approach. Indeed, an increase in tumor cell cytotoxicity was seen with this combination in wild-type MDA-MB-231 and MCF7; additive interactive killing was achieved, indicating the importance of the cholesterol uptake pathways. Our group next performed a double knock out of LDLR and SR-B1, which significantly hindered the cells' ability to take up LDL nanoparticles and impeded LDL-DHA-mediated killing of MDA-MB-231 cells; however, residual levels of LDL nanoparticle uptake and cytotoxicity were still active. This likely can be explained by LDLR/SR-B1 independent pathways, which may include: CD36,[74] lectin-type oxidized LDL receptor 1 (LOX-1),[75] activin-like kinase 1 (ALK1) receptor[76], and glycosaminoglycans (GAGs).[77] Each of these receptors has previously been shown to bind and take up native or modified LDL with varying affinities. Given that the conformation of apoB100 is retained in the LDL nanoparticles,[53] it is assumed that these nanoparticles may be able to interact with these receptors. To date, little is known about how LDL-DiI-OA/LDL-DHA nanoparticles interact with these cholesterol-importing receptors; however, this will be the subject of future studies.

The current study also investigated the anticancer utility of LDL-DHA nanoparticles across the panel of breast cancer cells. All breast cancer subtypes were documented to express both LDLR and SR-B1; in addition each cell was able to avidly take up LDL nanoparticles. The hormone-responsive and inflammatory tumor lines displayed a lower overall capacity for LDL nanoparticle uptake compared to the Her2+ and basal-like/Claudin-low lines, which were ~2-3-fold greater. With regards to cytotoxicity, the luminal and the Her2+ breast cancer lines displayed LD_{50s} ~30-52 μM, conversely, the basal-like/Claudin-low and inflammatory lines demonstrated increased sensitivity to LDL-DHA with LD_{50s} ~5-15 μM. While the tumor cell's capacity for LDL nanoparticle association is clearly an important contributor to LDL-DHA sensitivity (ie, high rates of LDL-DHA sensitivity are associated with high capacity for LDL nanoparticle uptake among basal-like/Claudin-low lines compared to hormone-responsive luminal lines), it is not the only determinant, as several cases did not follow this general trend. The Sum-149PT cells had low LDL nanoparticle binding/uptake, but displayed very high sensitivity to LDL-DHA; conversely, Her2+ SKBR3 showed high association for LDL nanoparticles, but only displayed moderate sensitivity to LDL-DHA. Additional cell-intrinsic factors are likely modulating the processing and metabolism of the acquired DHA. Given that DHA typically undergoes lipid peroxidation in malignant cells[69] the expression of antioxidant genes was explored in select breast cancer cells (MCF7, MDA-MB-231 and HCC1937). Lipid peroxidation actually decreased and remained unchanged for MCF7 and MDA-MB-231 cells, respectively, following LDL-DHA treatment. Both cell lines expressed ample amounts of free and lipid radical reducing antioxidants (SLC7A11, GCLC, GPX4, PRDX6, SOD1/2). Conversely, these antioxidants were minimally expressed in HCC1937 cells, thus sensitizing them to lipid peroxidation and DHA-mediated cell killing. Regardless of the induction of lipid peroxidation, we observed that nearly all breast cancer cells in our panel succumbed to apoptotic cell death after LDL-DHA treatment. The literature is replete with studies reporting DHA-mediated killing of breast cancer cells by apoptosis. DHA exerts its anti-proliferative and pro-apoptotic effects by altering various molecular pathways in breast cancer cells. One key mechanism is mediated through DHA's activation of PPARγ, which upregulates the plasma membrane presentation of the heparan sulfate proteoglycan, syndecan-1, a documented inducer of apoptosis.[46] At the metabolic level the oxidized derivative of DHA, 4-oxo-DHA, has been shown to be more potent at driving anti-proliferative pro-apoptotic effects against breast cancer cells than the parent molecule DHA.[78] Moreover, the 4-oxo-DHA metabolite displayed preferential cytotoxicity against basal breast cancer cell lines over luminal cell lines.[78] Similar differential sensitivities of breast cancer cells to LDL-DHA are reported in the present work. Further mechanistic studies by Chen et al went on to show that the actions of 4-oxo-DHA potently stimulate PPARɣ and 15-hydroxyprostaglandin dehydrogenase (15-PGDH) but suppress NF-κB, PI3K, and mTOR signaling.[79] These mechanisms are believed to drive the antitumor effects of DHA. Additional pro-apoptotic effects of DHA involve further modulation of survival mechanisms. The conventional mitogen-activated protein kinases (MAPKs) are also subject to DHA induction, where ERK/JNK/p38 expression is upregulated to provoke mitochondrial ROS and lipid peroxidation, triggering apoptosis.[80] In the ER, DHA has also been shown to decrease genes associated with cholesterol biosynthesis and increase genes in ER stress, which is known to drive apoptotic cell death.[81] Agnostic to DHAs specific path of apoptosis induction is the ultimate activation of extrinsic (increased death receptors TRAIL, DR4, and FAS) and intrinsic (depolarization of the mitochondrial membranes, decreased expression of Bcl-2, increased expression of Bax, activation of caspases notably −3, −7, and −9, and PARP cleavage) cell death pathways leading to apoptosis.

The cytotoxicity findings for LDL-DHA on SKBR3 were confounding as pronounced necrosis and minimal annexin V was reported for one assay, while significant activation of caspase activity was documented with another assay. It can be concluded that both cell death pathways are activated in this cell line in response to LDL-DHA. Elucidation of this mechanism remains a line for future investigation.

The present findings demonstrate the ability of LDL-DHA nanoparticles to effectively interact with cell surface LDLR and SR-B1 on breast cancer cells and subsequently deliver DHA into these cells. The internalized DHA was then shown to elicit cytotoxic effects on the breast cancer cells through the induction of apoptosis and necrosis pathways. The potential clinical relevance of this nanomedicine can be inferred from robust patient data regarding lipoprotein receptors in the setting of breast cancer. The early works of Rudling et al and others have documented that levels of LDLR in patient breast tumors inversely correlated with overall survival time.[4,82] More recently, SR-B1 has also been recognized to be upregulated in patient breast tumor tissue and is associated with malignant behaviors and poor survival.[39,40] These

studies collectively indicate that the more aggressive cases of breast cancer are associated with high LDLR and SR-B1 activity. Furthermore, complementary preclinical and epidemiological studies indicate that natural omega-3 fatty acids, such as DHA, elicit marked tumoricidal and anticancer effects on mammary malignancies.[66,83–85] Moreover, recent studies by Bobin-Dubigeon et al reported that plasma EPA/DHA associated with ApoB-containing lipoproteins correlated with reduced tumor proliferation in hormone receptor negative breast cancer patients.[68] It stands to reason, therefore, that the LDL-DHA nanotechnology may show considerable promise as a new therapeutic strategy against breast cancer. This is particularly pertinent as effective treatment options for aggressive breast tumors are limited.[86]

One should be aware that there are some caveats associated with the LDL-DHA nanomedicine approach. Namely, the high affinity of the LDL carrier for hepatic sequestration, which would limit the availability of the LDL nanoparticle at the target tumor site. This could be resolved with transarterial locoregional administration of LDL-DHA to the breast or metastatic site.[87,88] This would enable the first pass effects of the LDL nanoparticle to the tumor site to enable maximum tumor uptake with minimal systemic exposure. Secondary systemic exposure of LDL-DHA nanoparticles, however, is not a major concern, as our group has demonstrated these nanoparticles to be safe and well-tolerated by normal tissues.[42,89,90] In vivo studies to assess the therapeutic efficacy of LDL-DHA in local and metastatic breast cancer are actively being pursued in our group.

Other limitations of the current study include the small sample size of breast cancer cells for each molecular subtype. Future studies should involve a more extensive survey of cell lines for each molecular subtype. Evaluation of primary breast cancer cells or breast cancer organoids would also provide more clinically relevant assessments. In addition, a more thorough mechanistic elucidation of LDL-DHA breast cancer cytotoxicity is warranted. This could provide additional insights for potential drug combination treatment strategies.

Conclusion

In conclusion, we have shown that LDL-DHA nanoparticles avidly interact with both LDLR and SR-B1. This dual receptor targeting capability expands the receptor targeting purview of this LDL-based nanoparticle beyond LDLR. Given the essential role of cholesterol in mammalian cells, with malignant cells showing even higher cholesterol demands, LDLR and/or SR-B1 will be expressed at the cell surface of all cells, enabling LDL nanoparticle delivery. In light of this, the LDL-DHA nanoplatform could be viewed as a universal delivery system to mammalian cells. More specifically, in the present study, LDLR and SR-B1 expression were demonstrated across a panel of 10 breast cancer cells representative of all molecular subtypes. Regardless of receptor preference, dose-dependent LDL-DHA nanoparticle uptake was observed, and cytotoxicity was documented across all cells. Findings from our LDL-DHA nanoparticle construct are consistent with other reports in the field, highlighting that DHA administration is preferentially cytotoxic to basal/triple negative breast cancer cells over the luminal subtypes. Future studies will aim to validate the dual receptor targeting capabilities of LDL-DHA nanoparticles in in vivo rodent models of breast cancer. Additional studies should also demonstrate the preservation of this interaction across different tumor types, ie, document high uptake of LDL-DHA nanoparticles through LDLR and SR-B1 in different cancers. Finally, the ability of LDL-DHA nanoparticles to interact with other lipoprotein receptors (eg, ALK1, LOX, CD36, etc.) should be interrogated.

Data Sharing Statement

No datasets were generated or analyzed during the current study.

Acknowledgments

We acknowledge the aid given by the UT Southwestern flow cytometry core facility.

Author Contributions

All authors made a significant contribution to the work reported, whether that is in the conception, study design, execution, acquisition of data, analysis and interpretation or in all these areas; took part in drafting, revising or critically reviewing the article; gave final approval of the version to be published; have agreed on the journal to which the article has been submitted; and agree to be accountable for all aspects of the work.

Funding

This article was supported by the NCI, National Institute of Health under grants (R01CA215702, T32CA124334-13, R01CA271496), Society of Interventional Radiology Foundation Dr. Ernest J. Ring Academic Development Grant, and METAvivor research award.

Disclosure

Dr Ian Corbin reports a patent WO2014159851 A8 issued. The authors declare no other competing interests in this work.

References

1. Marino N, German R, Rao X, et al. Upregulation of lipid metabolism genes in the breast prior to cancer diagnosis. *Npj Breast Cancer*. 2020;6(1):50. doi:10.1038/s41523-020-00191-8
2. Zipinotti Dos Santos D, de Souza JC, Pimenta TM, et al. The impact of lipid metabolism on breast cancer: a review about its role in tumorigenesis and immune escape. *Cell Commun Signaling*. 2023;21(1):161. doi:10.1186/s12964-023-01178-1
3. Xiao Q, Xia M, Tang W, et al. The lipid metabolism remodeling: a hurdle in breast cancer therapy. *Cancer Lett*. 2024;582:216512. doi:10.1016/j.canlet.2023.216512
4. de Gonzalo-Calvo D, López-Vilaró L, Nasarre L, et al. Intratumor cholesteryl ester accumulation is associated with human breast cancer proliferation and aggressive potential: a molecular and clinicopathological study. *BMC Cancer*. 2015;15(1):460. doi:10.1186/s12885-015-1469-5
5. Cedó L, Reddy ST, Mato E, et al. HDL and LDL: potential New Players in Breast Cancer Development. *J Clin Med*. 2019;8(6):853. doi:10.3390/jcm8060853
6. Casaburi I, Chimento A, De Luca A, et al. Cholesterol as an Endogenous ERRalpha Agonist: a New Perspective to Cancer Treatment. *Front Endocrinol*. 2018;9:525. doi:10.3389/fendo.2018.00525
7. Maja M, Tyteca D. Alteration of cholesterol distribution at the plasma membrane of cancer cells: from evidence to pathophysiological implication and promising therapy strategy. *Front Physiol*. 2022;13:999883. doi:10.3389/fphys.2022.999883
8. Wallach EE, Shoham Z, Schachter M. Estrogen biosynthesis—regulation, action, remote effects, and value of monitoring in ovarian stimulation cycles. *Fertil Sterility*. 1996;65(4):687–701. doi:10.1016/S0015-0282(16)58197-7
9. Huang P, Nedelcu D, Watanabe M, et al. Cellular Cholesterol Directly Activates Smoothened in Hedgehog Signaling. *Cell*. 2016;166(5):1176–1187.e14. doi:10.1016/j.cell.2016.08.003
10. Wei W, Schwaid AG, Wang X, et al. Ligand Activation of ERRalpha by Cholesterol Mediates Statin and Bisphosphonate Effects. *Cell Metab*. 2016;23(3):479–491. doi:10.1016/j.cmet.2015.12.010
11. Nelson ER, Wardell SE, Jasper JS, et al. 27-Hydroxycholesterol Links Hypercholesterolemia and Breast Cancer Pathophysiology. *Science*. 2013;342(6162):1094. doi:10.1126/science.1241908
12. Pagliuca M, Donato M, D'Amato AL, et al. New steps on an old path: novel estrogen receptor inhibitors in breast cancer. *Crit Rev Oncol Hematol*. 2022;180:103861. doi:10.1016/j.critrevonc.2022.103861
13. Mollinedo F, Gajate C. Lipid rafts as major platforms for signaling regulation in cancer. *Adv Bio Regul*. 2015;57:130–146. doi:10.1016/j.jbior.2014.10.003
14. Irwin ME, Mueller KL, Bohin N, et al. Lipid raft localization of EGFR alters the response of cancer cells to the EGFR tyrosine kinase inhibitor gefitinib. *J Cell Physiol*. 2011;226(9):2316–2328. doi:10.1002/jcp.22570
15. Remacle-Bonnet M, Garrouste F, Baillat G, et al. Membrane rafts segregate pro- from anti-apoptotic insulin-like growth factor-I receptor signaling in colon carcinoma cells stimulated by members of the tumor necrosis factor superfamily. *Am J Pathol*. 2005;167(3):761–773. doi:10.1016/S0002-9440(10)62049-4
16. Pike LJ. The challenge of lipid rafts. *J Lipid Res*. 2009;50:S323–S328. doi:10.1194/jlr.R800040-JLR200
17. Zhang J, Li Q, Wu Y, et al. Cholesterol content in cell membrane maintains surface levels of ErbB2 and confers a therapeutic vulnerability in ErbB2-positive breast cancer. *Cell Commun Signaling*. 2019;17(1):15. doi:10.1186/s12964-019-0328-4
18. Ediriweera MK, Moon JY, Nguyen YT, et al. 10-Gingerol Targets Lipid Rafts Associated PI3K/Akt Signaling in Radio-Resistant Triple Negative Breast Cancer Cells. *Molecules*. 2020;25(14):3164. doi:10.3390/molecules25143164
19. Vona R, Iessi E, Matarrese P. Role of Cholesterol and Lipid Rafts in Cancer Signaling: a Promising Therapeutic Opportunity? *Front Cell Dev Biol*. 2021;9:622908. doi:10.3389/fcell.2021.622908
20. da Silva JL, Cardoso Nunes NC, Izetti P, et al. Triple negative breast cancer: a thorough review of biomarkers. *Crit Rev Oncol/Hematol*. 2020;145:102855. doi:10.1016/j.critrevonc.2019.102855
21. McCann KE, Hurvitz SA. Innovations in targeted therapies for triple negative breast cancer. *Curr Opin Obstet Gynecol*. 2021;33(1):34–47. doi:10.1097/GCO.0000000000000671
22. Nagy P, Vereb G, Sebestyén Z, et al. Lipid rafts and the local density of ErbB proteins influence the biological role of homo- and heteroassociations of ErbB2. *J Cell Sci*. 2002;115(Pt 22):4251–4262. doi:10.1242/jcs.00118
23. Calay D, Vind-Kezunovic D, Frankart A, et al. Inhibition of Akt signaling by exclusion from lipid rafts in normal and transformed epidermal keratinocytes. *J Invest Dermatol*. 2010;130(4):1136–1145. doi:10.1038/jid.2009.415
24. Huang B, B-l S, Xu C. Cholesterol metabolism in cancer: mechanisms and therapeutic opportunities. *Nat Metab*. 2020;2(2):132–141. doi:10.1038/s42255-020-0174-0
25. Borgquist S, Djerbi S, Pontén F, et al. HMG-CoA reductase expression in breast cancer is associated with a less aggressive phenotype and influenced by anthropometric factors. *Int J Cancer*. 2008;123(5):1146–1153. doi:10.1002/ijc.23597
26. Kim H, Seol YM, Choi YJ, et al. HMG CoA reductase expression as a prognostic factor in Korean patients with breast cancer: a retrospective study. *Medicine*. 2019;98(13):e14968. doi:10.1097/MD.0000000000014968
27. Sharma V, Sharma A. Serum cholesterol levels in carcinoma breast. *Indian J Med Res*. 1991;94:193–196.

28. Tulinius H, Sigfússon N, Sigvaldason H, et al. Risk factors for malignant diseases: a cohort study on a population of 22,946 Icelanders. *Cancer Epidemiol Biomarkers Prev*. 1997;6(11):863–873.
29. Bani IA, Williams CM, Boulter PS, et al. Plasma lipids and prolactin in patients with breast cancer. *Br J Cancer*. 1986;54(3):439–446. doi:10.1038/bjc.1986.195
30. Markel A, Brook G. Cancer and hypocholesterolemia Isr J Med Sci. 1994 30(10)787–793.
31. Peterson C, Vitols S, Rudling M, et al. Hypocholesterolemia in cancer patients may be caused by elevated LDL receptor activities in malignant cells. *Medical Oncology Tumor Pharmacother*. 1985;2(3):143–147. doi:10.1007/BF02934541
32. Vitols S, Gahrton G, Bjorkholm M, et al. Hypocholesterolaemia in malignancy due to elevated low-density-lipoprotein-receptor activity in tumour cells: evidence from studies in patients with leukaemia. *Lancet*. 1985;2(8465):1150–1154. doi:10.1016/S0140-6736(85)92679-0
33. Alexopoulos CG, Pournaras S, Vaslamatzis M, et al. Changes in serum lipids and lipoproteins in cancer patients during chemotherapy. *Cancer Chemother Pharmacol*. 1992;30(5):412–416. doi:10.1007/BF00689971
34. Tulenko TN, Sumner AE. The physiology of lipoproteins. *J Nucl Cardiol*. 2002;9(6):638–649. doi:10.1067/mnc.2002.128959
35. Pires LA, Hegg R, Freitas FR, et al. Effect of neoadjuvant chemotherapy on low-density lipoprotein (LDL) receptor and LDL receptor-related protein 1 (LRP-1) receptor in locally advanced breast cancer. *Braz J Med Biol Res*. 2012;45(6):557–564. doi:10.1590/S0100-879X2012007500068
36. Cao WM, Murao K, Imachi H, et al. A mutant high-density lipoprotein receptor inhibits proliferation of human breast cancer cells. *Cancer Res*. 2004;64(4):1515–1521. doi:10.1158/0008-5472.CAN-03-0675
37. Gallagher EJ, Zelenko Z, Neel BA, et al. Elevated tumor LDLR expression accelerates LDL cholesterol-mediated breast cancer growth in mouse models of hyperlipidemia. *Oncogene*. 2017;36(46):6462–6471. doi:10.1038/onc.2017.247
38. Rotheneder M, Kostner GM. Effects of low- and high-density lipoproteins on the proliferation of human breast cancer cells in vitro: differences between hormone-dependent and hormone-independent cell lines. *Int J Cancer*. 1989;43(5):875–879. doi:10.1002/ijc.2910430523
39. Yuan B, Wu C, Wang X, et al. High scavenger receptor class B type I expression is related to tumor aggressiveness and poor prognosis in breast cancer. *Tumour Biol*. 2016;37(3):3581–3588. doi:10.1007/s13277-015-4141-4
40. Li J, Wang J, Li M, et al. Up-regulated expression of scavenger receptor class B type 1 (SR-B1) is associated with malignant behaviors and poor prognosis of breast cancer. *Pathol Res Pract*. 2016;212(6):555–559. doi:10.1016/j.prp.2016.03.011
41. Wang Y, Li J, Do Vale GD, et al. Repeated trans-arterial treatments of LDL-DHA nanoparticles induce multiple pathways of tumor cell death in hepatocellular carcinoma bearing rats. *Front Oncol*. 2022;12:1052221. doi:10.3389/fonc.2022.1052221
42. Li J, Canseco D, Wang Y, et al. Assessing the safety of transarterial locoregional delivery of low-density lipoprotein docosahexaenoic acid nanoparticles to the rat liver. *Eur J Pharm Biopharm*. 2021;158:273–283. doi:10.1016/j.ejpb.2020.10.018
43. Blanckaert V, Ulmann L, Mimouni V, et al. Docosahexaenoic acid intake decreases proliferation, increases apoptosis and decreases the invasive potential of the human breast carcinoma cell line MDA-MB-231. *Int J Oncol*. 2010;36(3):737–742. doi:10.3892/ijo_00000549
44. Ravacci GR, Brentani MM, Tortelli TC, et al. Docosahexaenoic Acid Modulates a HER2-Associated Lipogenic Phenotype, Induces Apoptosis, and Increases Trastuzumab Action in HER2-Overexpressing Breast Carcinoma Cells. *Biomed Res Int*. 2015;2015:838652. doi:10.1155/2015/838652
45. Xue M, Ge Y, Yu C, et al. Apoptosis is induced by docosahexaenoic acid in breast cancer cells via death receptor and mitochondria-mediated pathways. *Mol Med Rep*. 2017;16(1):978–982. doi:10.3892/mmr.2017.6678
46. Sun H, Berquin IM, Owens RT, et al. Peroxisome proliferator-activated receptor gamma-mediated up-regulation of syndecan-1 by n-3 fatty acids promotes apoptosis of human breast cancer cells. *Cancer Res*. 2008;68(8):2912–2919. doi:10.1158/0008-5472.CAN-07-2305
47. Edwards IJ, Berquin IM, Sun H, et al. Differential effects of delivery of omega-3 fatty acids to human cancer cells by low-density lipoproteins versus albumin. *Clin Cancer Res*. 2004;10(24):8275–8283. doi:10.1158/1078-0432.CCR-04-1357
48. Lund-Katz S, Laplaud PM, Phillips MC, et al. Apolipoprotein B-100 conformation and particle surface charge in human LDL subspecies: implication for LDL receptor interaction. *Biochemistry*. 1998;37(37):12867–12874. doi:10.1021/bi980828m
49. Havel RJ, Eder HA, Bragdon JH. The distribution and chemical composition of ultracentrifugally separated lipoproteins in human serum. *J Clin Invest*. 1955;34(9):1345–1353. doi:10.1172/JCI103182
50. Zimetti F, Weibel GK, Duong M, et al. Measurement of cholesterol bidirectional flux between cells and lipoproteins. *J Lipid Res*. 2006;47(3):605–613. doi:10.1194/jlr.M500466-JLR200
51. Mulik RS, Zheng H, Pichumani K, et al. Elucidating the structural organization of a novel low-density lipoprotein nanoparticle reconstituted with docosahexaenoic acid. *Chem Phys Lipids*. 2017;204:65–75. doi:10.1016/j.chemphyslip.2017.03.007
52. Li H, Z Z, B D, et al. Carbocyanine labeled LDL for optical imaging of tumors. *Acad Radiol*. 2004;11(6):669–677. doi:10.1016/j.acra.2004.01.016
53. Reynolds L, Mulik RS, Wen X, et al. Low-density lipoprotein-mediated delivery of docosahexaenoic acid selectively kills murine liver cancer cells. *Nanomedicine*. 2014;9(14):2123–2141. doi:10.2217/nnm.13.187
54. Zheng SQ, Palovcak E, Armache J-P, et al. MotionCor2: anisotropic correction of beam-induced motion for improved cryo-electron microscopy. *Nature Methods*. 2017;14(4):331–332. doi:10.1038/nmeth.4193
55. Tan YZ, Baldwin PR, Davis JH, et al. Addressing preferred specimen orientation in single-particle cryo-EM through tilting. *Nature Methods*. 2017;14(8):793–796. doi:10.1038/nmeth.4347
56. Tang G, Peng L, Baldwin PR, et al. EMAN2: an extensible image processing suite for electron microscopy. *J Struct Biol*. 2007;157(1):38–46. doi:10.1016/j.jsb.2006.05.009
57. Acton SL, Scherer PE, Lodish HF, et al. Expression cloning of SR-B1, a CD36-related class B scavenger receptor. *J Biol Chem*. 1994;269(33):21003–21009. doi:10.1016/S0021-9258(17)31921-X
58. Stangl H, Hyatt M, Hobbs HH. Transport of lipids from high and low density lipoproteins via scavenger receptor-BI. *J Biol Chem*. 1999;274(46):32692–32698. doi:10.1074/jbc.274.46.32692
59. Basak JM, Verghese PB, Yoon H, et al. Low-density Lipoprotein Receptor Represents an Apolipoprotein E-independent Pathway of Aβ Uptake and Degradation by Astrocytes*. *J Biol Chem*. 2012;287(17):13959–13971. doi:10.1074/jbc.M111.288746
60. Gillard BK, Bassett GR, Gotto Jr AM, et al. Scavenger receptor B1 (SR-B1) profoundly excludes high density lipoprotein (HDL) apolipoprotein AII as it nibbles HDL-cholesteryl ester. *J Biol Chem*. 2017;292(21):8864–8873. doi:10.1074/jbc.M117.781963
61. Scully T, Kase N, Gallagher EJ, et al. Regulation of low-density lipoprotein receptor expression in triple negative breast cancer by EGFR-MAPK signaling. *Sci Rep*. 2021;11(1):17927. doi:10.1038/s41598-021-97327-y

62. Nikanjam M, Gibbs AR, Hunt CA, et al. Synthetic nano-LDL with paclitaxel oleate as a targeted drug delivery vehicle for glioblastoma multiforme. *J Control Release*. 2007;124(3):163–171. doi:10.1016/j.jconrel.2007.09.007
63. Ye J, Xia X, Dong W, et al. Cellular uptake mechanism and comparative evaluation of antineoplastic effects of paclitaxel-cholesterol lipid emulsion on triple-negative and non-triple-negative breast cancer cell lines. *Int J Nanomed*. 2016;11:4125–4140. doi:10.2147/IJN.S113638
64. Pan H, Sun Y, Cao D, et al. Low-density lipoprotein decorated and indocyanine green loaded silica nanoparticles for tumor-targeted photothermal therapy of breast cancer. *Pharm Dev Technol*. 2020;25(3):308–315. doi:10.1080/10837450.2019.1684944
65. Masquelier M, Vitols S, Pålsson M, et al. Low Density Lipoprotein as a Carrier of Cytostatics in Cancer Chemotherapy: study of Stability of Drug-carrier Complexes in Blood. *J Drug Targeting*. 2000;8(3):155–164. doi:10.3109/10611860008996861
66. Zheng JS, Hu XJ, Zhao YM, et al. Intake of fish and marine n-3 polyunsaturated fatty acids and risk of breast cancer: meta-analysis of data from 21 independent prospective cohort studies. *BMJ*. 2013;346(jun27 5):f3706. doi:10.1136/bmj.f3706
67. Patterson RE, Flatt SW, Newman VA, et al. Marine fatty acid intake is associated with breast cancer prognosis. *J Nutr*. 2011;141(2):201–206. doi:10.3945/jn.110.128777
68. Bobin-Dubigeon C, Nazih H, Croyal M, et al. Link between Omega 3 Fatty Acids Carried by Lipoproteins and Breast Cancer Severity. *Nutrients*. 2022;14(12):2461. doi:10.3390/nu14122461
69. Moss LR, Mulik RS, Van Treuren T, et al. Investigation into the distinct subcellular effects of docosahexaenoic acid loaded low-density lipoprotein nanoparticles in normal and malignant murine liver cells. *Biochim Biophys Acta*. 2016;1860(11):2363–2376. doi:10.1016/j.bbagen.2016.07.004
70. He B, Yang Q. Recent Development of LDL-Based Nanoparticles for Cancer Therapy. *Pharmaceuticals*. 2022;16(1):18. doi:10.3390/ph16010018
71. Glass C, Pittman RC, Weinstein DB, et al. Dissociation of tissue uptake of cholesterol ester from that of apoprotein A-I of rat plasma high density lipoprotein: selective delivery of cholesterol ester to liver, adrenal, and gonad. *Proc Natl Acad Sci*. 1983;80(17):5435–5439. doi:10.1073/pnas.80.17.5435
72. Rigotti A, Acton SL, Krieger M. The Class B Scavenger Receptors SR-B1 and CD36 Are Receptors for Anionic Phospholipids. *J Biol Chem*. 1995;270(27):16221–16224. doi:10.1074/jbc.270.27.16221
73. Yamamoto S, Fukuhara T, Ono C, et al. Lipoprotein Receptors Redundantly Participate in Entry of Hepatitis C Virus. *Plos Pathog*. 2016;12(5):e1005610. doi:10.1371/journal.ppat.1005610
74. Calvo D, Gómez-Coronado D, Suárez Y, et al. Human CD36 is a high affinity receptor for the native lipoproteins HDL, LDL, and VLDL. *J Lipid Res*. 1998;39(4):777–788. doi:10.1016/S0022-2275(20)32566-9
75. Chen M, Masaki T, Sawamura T. LOX-1, the receptor for oxidized low-density lipoprotein identified from endothelial cells: implications in endothelial dysfunction and atherosclerosis. *Pharmacol Ther*. 2002;95(1):89–100. doi:10.1016/S0163-7258(02)00236-X
76. Kraehling JR, Chidlow JH, Rajagopal C, et al. Genome-wide RNAi screen reveals ALK1 mediates LDL uptake and transcytosis in endothelial cells. *Nat Commun*. 2016;7(1):13516. doi:10.1038/ncomms13516
77. Olsson U, Ostergren-Lundén G, Moses J. Glycosaminoglycan-lipoprotein interaction. *Glycoconjugate J*. 2001;18(10):789–797. doi:10.1023/A:1021155518464
78. Pogash TJ, El-Bayoumy K, Amin S, et al. Oxidized derivative of docosahexaenoic acid preferentially inhibit cell proliferation in triple negative over luminal breast cancer cells. *Vitro Cell Dev Biol Anim*. 2015;51(2):121–127. doi:10.1007/s11626-014-9822-6
79. Chen KM, Thompson H, Vanden-Heuvel JP, et al. Lipoxygenase catalyzed metabolites derived from docosahexaenoic acid are promising antitumor agents against breast cancer. *Sci Rep*. 2021;11(1):410. doi:10.1038/s41598-020-79716-x
80. Jeong S, Jing K, Kim N, et al. Docosahexaenoic acid-induced apoptosis is mediated by activation of mitogen-activated protein kinases in human cancer cells. *BMC Cancer*. 2014;14(1):481. doi:10.1186/1471-2407-14-481
81. Chénais B, Cornec M, Dumont S, et al. Transcriptomic Response of Breast Cancer Cells MDA-MB-231 to Docosahexaenoic Acid: downregulation of Lipid and Cholesterol Metabolism Genes and Upregulation of Genes of the Pro-Apoptotic ER-Stress Pathway. *Int J Environ Res Public Health*. 2020;17(10):3746. doi:10.3390/ijerph17103746
82. Rudling MJ, Stahle L, Peterson CO, et al. Content of low density lipoprotein receptors in breast cancer tissue related to survival of patients. *Br Med J*. 1986;292(6520):580–582. doi:10.1136/bmj.292.6520.580
83. Jiang W, Zhu Z, McGinley JN, et al. Identification of a molecular signature underlying inhibition of mammary carcinoma growth by dietary N-3 fatty acids. *Cancer Res*. 2012;72(15):3795–3806. doi:10.1158/0008-5472.CAN-12-1047
84. MacLennan MB, Clarke SE, Perez K, et al. Mammary tumor development is directly inhibited by lifelong n-3 polyunsaturated fatty acids. *J Nutr Biochem*. 2013;24(1):388–395. doi:10.1016/j.jnutbio.2012.08.002
85. Yang B, Ren XL, Fu YQ, et al. Ratio of n-3/n-6 PUFAs and risk of breast cancer: a meta-analysis of 274135 adult females from 11 independent prospective studies. *BMC Cancer*. 2014;14(1):105. doi:10.1186/1471-2407-14-105
86. Zhu S, Wu Y, Song B, et al. Recent advances in targeted strategies for triple-negative breast cancer. *J hematol oncol*. 2023;16(1):100.
87. Deipolyi AR, Ward RC, Riaz A, et al. Locoregional Therapies for Primary and Metastatic Breast Cancer: AJR Expert Panel Narrative Review. *Am J Roentgenol*. 2024;222(2):e2329454. doi:10.2214/AJR.23.29454
88. Hori A, Kennoki N, Hori S, et al. Feasibility Study of Transarterial Chemotherapy Followed by Chemoembolization for Recurrent Breast Cancer. *J Vasc Interv Radiol*. 2024;35(4):516–522. doi:10.1016/j.jvir.2023.12.016
89. Wang Y, Li J, Subramaniyan I, et al. An implanted port-catheter system for repeated hepatic arterial infusion of low-density lipoprotein-docosahexaenoic acid nanoparticles in normal rats: a safety study. *Toxicol Appl Pharmacol*. 2020;400:115037. doi:10.1016/j.taap.2020.115037
90. Mulik RS, Bing C, Ladouceur-Wodzak M, et al. Localized delivery of low-density lipoprotein docosahexaenoic acid nanoparticles to the rat brain using focused ultrasound. *Biomaterials*. 2016;83:257–268. doi:10.1016/j.biomaterials.2016.01.021